Supporting Information for “Layer Charge Effects on Adsorption and Diffusion of Water and Ions in Interlayers and on External Surfaces of Montmorillonite”

Yafan Yang, Arun Kumar Narayanan Nair,*

and Shuyu Sun

Physical Science and Engineering Division (PSE),

Computational Transport Phenomena Laboratory,

King Abdullah University of Science and Technology (KAUST),

Thuwal, 23955-6900, Saudi Arabia.

October 28, 2019

*To whom correspondence should be addressed, email: arun.narayanannair@kaust.edu.sa

Table S1: BET constant (c) and monolayer capacity (v_{m}) for Arizona samples at $T = 298.15$ K. The basal $d-$spacing is fixed at 65 Å.

Clay type	v_{m} (per $O_{20}(OH)_4$)	c
Li-montmorillonite	6.53	55.39
Na-montmorillonite	5.45	134.16
K-montmorillonite	5.78	96.74
Mg-montmorillonite	9.15	396.54
Ca-montmorillonite	9.93	152.42
Sr-montmorillonite	8.52	325.23

Table S2: Diffusion coefficients (D_{xy}) of the different species in the interlayers of Arizona samples saturated with monovalent cations at $T = 298.15$ K. The basal $d-$spacings are as given in Table 2.

Clay type	RH (%)	Diffusion coefficient ($10^{-11}m^2/s$)	
		Ion	H_2O
Li-montmorillonite	1 (1W)	0.21 ± 0.047	0.84 ± 0.16
	5 (1W)	0.19 ± 0.032	1.02 ± 0.10
	10 (1W)	0.14 ± 0.041	1.09 ± 0.22
	40 (1W)	0.11 ± 0.032	1.15 ± 0.13
	45 (1W)	0.094 ± 0.029	1.40 ± 0.21
	50 (1W)	0.11 ± 0.026	1.31 ± 0.21
	80 (2W)	16.10 ± 2.70	48.09 ± 2.65
	90 (2W)	15.80 ± 3.52	47.53 ± 2.99
	12 (1W) [a]	5.7	–
	85 (2W) [a]	68.4	–
Na-montmorillonite	40 (1W)	9.46 ± 1.08	26.34 ± 3.28
	45 (1W)	8.23 ± 9.82	24.80 ± 2.27
	50 (1W)	9.80 ± 1.04	26.22 ± 0.85
	80 (2W)	35.60 ± 3.42	98.94 ± 3.22
	90 (2W)	42.80 ± 6.52	102.22 ± 36.30
	30 (1W) [a]	5.4	–
	90 (2W) [a]	96.0	–
	43 (1W) [b]	–	10.0−30.0
	85 (2W) [b]	–	50.0−100.0
	- (1W) [c]	16.0	46.0
	- (2W) [c]	51.0	131.0
K-montmorillonite	40 (1W)	4.22 ± 0.78	42.19 ± 1.91
	45 (1W)	4.55 ± 0.88	37.35 ± 2.05
	50 (1W)	4.27 ± 0.56	41.68 ± 4.16
	80 (1W)	4.32 ± 0.85	35.59 ± 1.93
	90 (1W)	4.62 ± 0.99	38.52 ± 3.78
	25 (1W) [a]	21.5	–

[a]Experimental studies of Salles et al., 2015. [b]Experimental studies of Malikova et al., 2006. [c]Simulation studies of Greathouse et al., 2016.

Table S3: Diffusion coefficients (D_{xy}) of the different species in the interlayers of Arizona samples saturated with divalent cations at $T = 298.15$ K. The basal $d-$spacings are as given in Table 2.

Clay type	RH (%)	Diffusion coefficient ($10^{-11} m^2/s$)	
		Ion	H_2O
Mg-montmorillonite	1 (1W)	0.018 ± 0.020	8.09 ± 0.56
	5 (1W)	0.026 ± 0.013	12.01 ± 3.18
	10 (1W)	0.019 ± 0.011	8.22 ± 1.26
	40 (2W)	3.39 ± 0.49	48.62 ± 1.65
	45 (2W)	3.65 ± 0.87	47.03 ± 2.80
	50 (2W)	3.75 ± 0.75	47.51 ± 1.44
	80 (2W)	3.51 ± 0.53	45.02 ± 1.67
	90 (2W)	3.83 ± 1.18	45.47 ± 4.20
Ca-montmorillonite	1 (1W)	0.031 ± 0.026	7.14 ± 1.80
	5 (1W)	0.050 ± 0.042	8.73 ± 1.08
	10 (1W)	0.035 ± 0.015	9.02 ± 1.53
	40 (2W)	0.58 ± 0.23	48.56 ± 2.26
	45 (2W)	0.55 ± 0.46	49.01 ± 2.57
	50 (2W)	0.59 ± 0.39	47.62 ± 2.35
	80 (2W)	0.55 ± 0.28	45.38 ± 2.78
	90 (2W)	0.46 ± 0.05	45.32 ± 1.31
Sr-montmorillonite	1 (1W)	0.064 ± 0.015	24.6 ± 5.07
	5 (1W)	0.095 ± 0.055	18.52 ± 2.32
	10 (1W)	0.092 ± 0.044	17.68 ± 1.97
	40 (2W)	2.25 ± 0.71	50.59 ± 2.00
	45 (2W)	2.27 ± 0.47	47.61 ± 1.26
	50 (2W)	2.06 ± 0.83	48.32 ± 1.76
	80 (2W)	2.43 ± 0.58	46.91 ± 1.52
	90 (2W)	2.57 ± 0.78	48.83 ± 2.11

Table S4: Diffusion coefficients (D_{xy}) of the different species in Arizona samples saturated with monovalent cations at T = 298.15 K. The basal $d-$spacing is fixed at 65 Å.

Clay type	RH (%)	Diffusion coefficient ($10^{-11}m^2/s$)	
		Ion	H_2O
Li-montmorillonite	1	0.11 ± 0.084	19.32 ± 11.11
	20	23.03 ± 3.60	154.21 ± 21.03
	40	47.01 ± 17.52	156.32 ± 24.45
	60	41.39 ± 24.73	178.93 ± 14.70
	80	43.16 ± 7.18	217.12 ± 22.71
	≈ 100	91.56 ± 46.60	321.23 ± 16.52
Na-montmorillonite	1	4.14 ± 2.62	209.43 ± 44.41
	20	37.61 ± 8.99	243.55 ± 28.71
	40	58.88 ± 17.11	232.12 ± 31.42
	60	81.87 ± 32.62	259.03 ± 18.94
	80	113.87 ± 38.70	271.08 ± 14.29
	≈ 100	117.12 ± 29.30	333.41 ± 17.71
K-montmorillonite	1	0.014 ± 0.011	138.79 ± 56.71
	20	8.57 ± 3.48	313.23 ± 57.42
	40	12.81 ± 4.42	284.12 ± 36.02
	60	26.29 ± 8.26	306.45 ± 49.91
	80	31.11 ± 24.14	280.65 ± 37.43
	≈ 100	127.95 ± 46.01	337.11 ± 21.31

Table S5: Diffusion coefficients (D_{xy}) of the different species in Arizona samples saturated with divalent cations at T = 298.15 K. The basal d−spacing is fixed at 65 Å.

Clay type	RH (%)	Diffusion coefficient ($10^{-11} m^2/s$)	
		Ion	H_2O
Mg-montmorillonite	1	0.058 ± 0.042	90.11 ± 16.10
	20	10.89 ± 3.51	157.12 ± 16.61
	40	15.84 ± 8.18	193.01 ± 27.82
	60	20.42 ± 14.21	206.99 ± 21.21
	80	28.51 ± 9.91	243.02 ± 21.09
	≈ 100	98.48 ± 57.66	319 ± 21.8
Ca-montmorillonite	1	3.13 ± 2.68	90.42 ± 17.08
	20	18.81 ± 10.69	190.99 ± 23.28
	40	18.22 ± 10.89	196.79 ± 11.29
	60	30.19 ± 24.51	207.21 ± 25.51
	80	41.68 ± 11.92	246.33 ± 22.53
	≈ 100	88.69 ± 28.72	319.01 ± 21.90
Sr-montmorillonite	1	0.098 ± 0.015	130.99 ± 26.01
	20	23.62 ± 11.71	185.88 ± 23.02
	40	27.23 ± 7.80	207.98 ± 14.89
	60	32.92 ± 20.43	224.12 ± 17.59
	80	31.61 ± 22.01	226.21 ± 21.80
	≈ 100	47.96 ± 21.28	320.03 ± 18.41

Table S6: Approximate RH ranges and the corresponding hydration states/basal $d-$spacings observed experimentally and employed in our simulations for Wyoming montmorillonite in contact with water at $T = 298.15$ K.

Clay type	RH (%)	hydration state/basal $d-$spacing	
		Experiment [a]	Simulation (Å) [b]
Li-montmorillonite	0 – 60	1W	12.0
	60 – 100	2W	15.0
Na-montmorillonite	0 – 20	0W	10.0
	20 – 60	1W	12.0
	60 – 100	2W	15.0
K-montmorillonite	0 – 20	0W	10.0
	20 – 100	1W	12.0
Mg-montmorillonite	0 – 20	1W	12.0
	20 – 100	2W	15.0
Ca-montmorillonite	0 – 20	1W	12.0
	20 – 100	2W	15.0
Sr-montmorillonite	0 – 40	1W	12.0
	40 – 100	2W	15.0

[a]Experimental studies of Ferrage et al., 2005. [b]Simulation studies of Li et al., 2019.

Table S7: Diffusion coefficients (D_{xy}) of the different species in the interlayers of Wyoming samples saturated with monovalent cations at T = 298.15 K. The basal $d-$spacings are as given in Table S6.

Clay type	RH (%)	Diffusion coefficient ($10^{-11} m^2/s$)	
		Ion	H_2O
Li-montmorillonite	1 (1W)	0.23 ± 0.077	6.58 ± 1.05
	5 (1W)	0.25 ± 0.085	8.48 ± 1.04
	10 (1W)	0.23 ± 0.062	9.49 ± 1.05
	40 (1W)	0.14 ± 0.024	11.61 ± 2.13
	45 (1W)	0.20 ± 0.084	13.83 ± 2.19
	50 (1W)	0.17 ± 0.045	12.91 ± 1.30
	80 (2W)	23.61 ± 4.70	93.89 ± 8.22
	90 (2W)	22.92 ± 4.49	95.91 ± 4.23
Na-montmorillonite	40 (1W)	3.55 ± 1.22	41.50 ± 3.25
	45 (1W)	3.27 ± 1.24	42.72 ± 2.42
	50 (1W)	2.89 ± 0.40	37.91 ± 3.31
	80 (2W)	34.03 ± 2.59	141.98 ± 6.81
	90 (2W)	37.91 ± 5.10	145.78 ± 11.02
K-montmorillonite	40 (1W)	4.32 ± 0.83	70.88 ± 4.48
	45 (1W)	4.14 ± 1.33	72.22 ± 6.20
	50 (1W)	4.62 ± 0.90	68.53 ± 3.80
	80 (1W)	5.30 ± 1.34	72.11 ± 2.18
	90 (1W)	5.59 ± 1.06	73.25 ± 6.05

Table S8: Diffusion coefficients (D_{xy}) of the different species in the interlayers of Wyoming samples saturated with divalent cations at T = 298.15 K. The basal $d-$spacings are as given in Table S6.

Clay type	RH (%)	Diffusion coefficient ($10^{-11}m^2/s$)	
		Ion	H_2O
Mg-montmorillonite	1 (1W)	0.0079 ± 0.0060	12.3 ± 2.53
	5 (1W)	0.016 ± 0.010	19.01 ± 4.23
	10 (1W)	0.013 ± 0.015	17.62 ± 1.48
	40 (2W)	2.76 ± 0.97	90.23 ± 7.61
	45 (2W)	3.28 ± 1.89	86.41 ± 4.45
	50 (2W)	2.25 ± 0.93	81.90 ± 6.05
	80 (2W)	2.26 ± 0.50	83.09 ± 4.96
	90 (2W)	2.16 ± 0.56	79.66 ± 3.43
Ca-montmorillonite	1 (1W)	0.022 ± 0.035	7.05 ± 0.82
	5 (1W)	0.036 ± 0.024	12.46 ± 0.83
	10 (1W)	0.026 ± 0.020	15.17 ± 1.19
	40 (2W)	3.00 ± 1.55	99.82 ± 4.16
	45 (2W)	3.59 ± 1.85	98.66 ± 2.98
	50 (2W)	3.08 ± 1.49	96.21 ± 5.21
	80 (2W)	2.67 ± 1.37	95.07 ± 4.85
	90 (2W)	2.99 ± 1.20	95.36 ± 4.63
Sr-montmorillonite	1 (1W)	0.10 ± 0.091	18.1 ± 1.99
	5 (1W)	0.15 ± 0.073	27.02 ± 2.92
	10 (1W)	0.12 ± 0.081	24.41 ± 1.17
	40 (2W)	4.34 ± 1.23	102.11 ± 3.83
	45 (2W)	3.69 ± 1.15	101.14 ± 4.35
	50 (2W)	3.51 ± 2.05	95.91 ± 2.89
	80 (2W)	3.85 ± 1.94	97.62 ± 8.28
	90 (2W)	4.04 ± 1.60	94.63 ± 4.45

Table S9: Diffusion coefficients (D_{xy}) of the different species in Wyoming samples saturated with monovalent cations at T = 298.15 K. The basal $d-$spacing is fixed at 65 Å.

Clay type	RH (%)	Diffusion coefficient ($10^{-11} m^2/s$)	
		Ion	H_2O
Li-montmorillonite	1	1.26 ± 1.58	17.41 ± 14.52
	20	37.03 ± 19.39	178.88 ± 37.41
	40	24.94 ± 8.90	229.89 ± 24.51
	60	37.47 ± 14.74	278.14 ± 43.44
	80	48.12 ± 17.31	324.67 ± 41.53
	≈ 100	89.42 ± 27.03	329.12 ± 9.23
Na-montmorillonite	1	6.39 ± 3.12	59.01 ± 9.79
	20	19.21 ± 11.47	223.77 ± 67.52
	40	31.52 ± 20.43	274.45 ± 67.44
	60	48.21 ± 25.19	309.13 ± 21.63
	80	58.60 ± 17.81	318.21 ± 38.42
	≈ 100	96.79 ± 32.04	333.89 ± 13.71
K-montmorillonite	1	0.72 ± 1.22	68.61 ± 57.23
	20	7.73 ± 6.08	159.97 ± 37.61
	40	7.79 ± 12.27	243.12 ± 69.93
	60	17.80 ± 12.01	304.67 ± 52.94
	80	22.32 ± 10.29	365.68 ± 74.91
	≈ 100	119 ± 62.01	360.69 ± 27.02

Table S10: Diffusion coefficients (D_{xy}) of the different species in Wyoming samples saturated with divalent cations at T = 298.15 K. The basal $d-$spacing is fixed at 65 Å.

Clay type	RH (%)	Diffusion coefficient ($10^{-11}m^2/s$)	
		Ion	H_2O
Mg-montmorillonite	1	0.66 ± 1.26	40.59 ± 22.59
	20	5.14 ± 6.22	178.98 ± 32.01
	40	7.38 ± 7.75	234.12 ± 19.10
	60	7.66 ± 3.33	239.21 ± 28.08
	80	14.17 ± 10.34	280.31 ± 41.42
	≈ 100	31.00 ± 10.62	316.97 ± 7.15
Ca-montmorillonite	1	2.92 ± 1.96	93.41 ± 41.03
	20	7.46 ± 5.91	241.22 ± 39.82
	40	5.16 ± 4.42	258.12 ± 34.21
	60	9.69 ± 7.89	274.03 ± 46.00
	80	22.81 ± 13.12	271.98 ± 31.43
	≈ 100	37.04 ± 22.74	318.15 ± 11.93
Sr-montmorillonite	1	0.74 ± 1.53	72.81 ± 20.48
	20	13.41 ± 8.09	255.96 ± 45.62
	40	18.04 ± 10.32	272.76 ± 41.93
	60	13.40 ± 5.45	289.01 ± 37.22
	80	19.93 ± 10.47	286.23 ± 15.19
	≈ 100	32.83 ± 12.58	310.25 ± 9.88

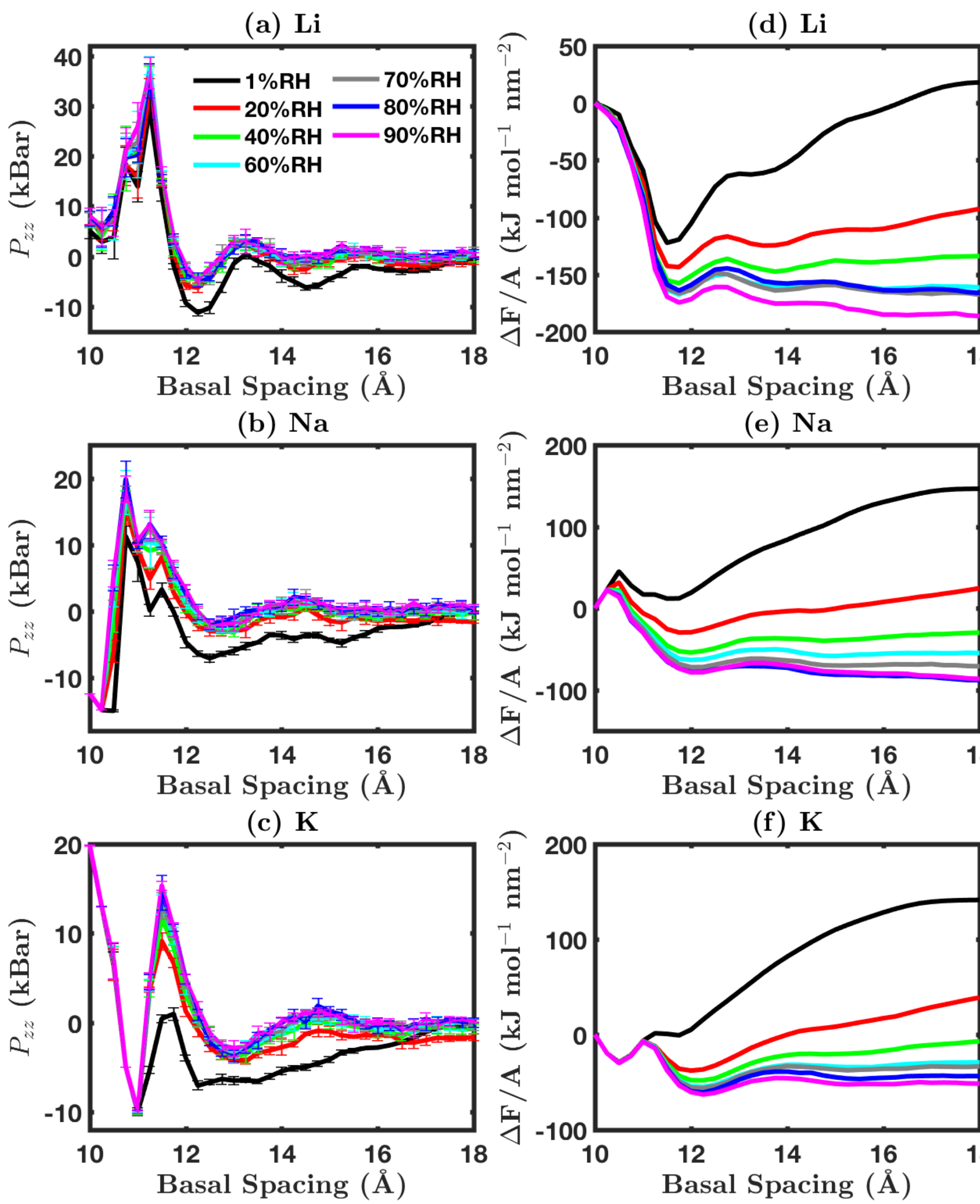

Figure S1: Variations of normal pressure P_{zz} (left panels) and swelling free energy per clay platelet area $\Delta F/A$ (right panels) as a function of the basal $d-$spacing of Arizona samples saturated with monovalent ions at T = 298.15 K. Simulations are performed under different RH conditions. (a,d) Li-, (b,e) Na-, and (c,f) K-montmorillonite.

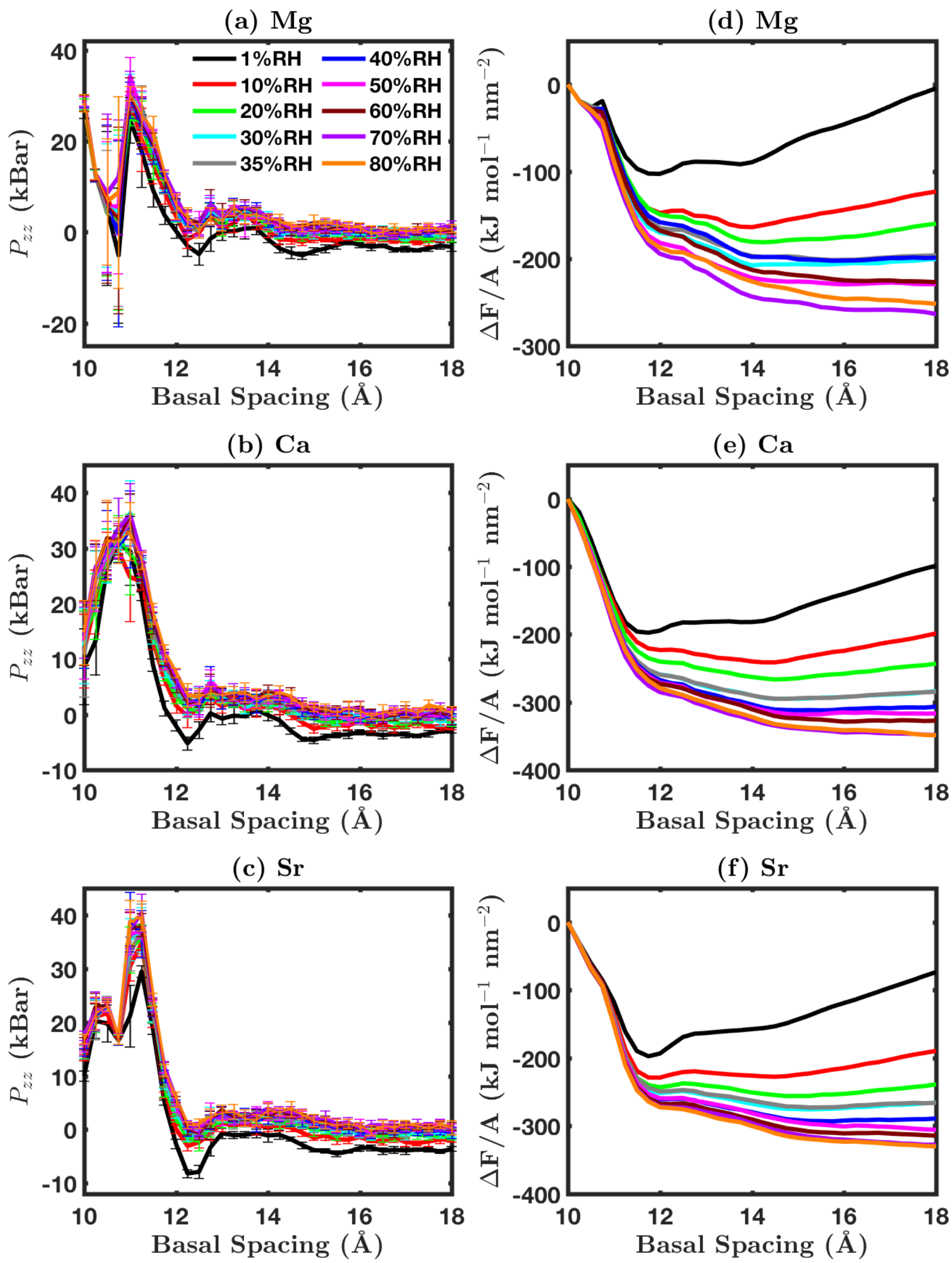

Figure S2: Same as in Fig. S1, but for samples saturated with divalent ions. (a,d) Mg-, (b,e) Ca-, and (c,f) Sr-montmorillonite.

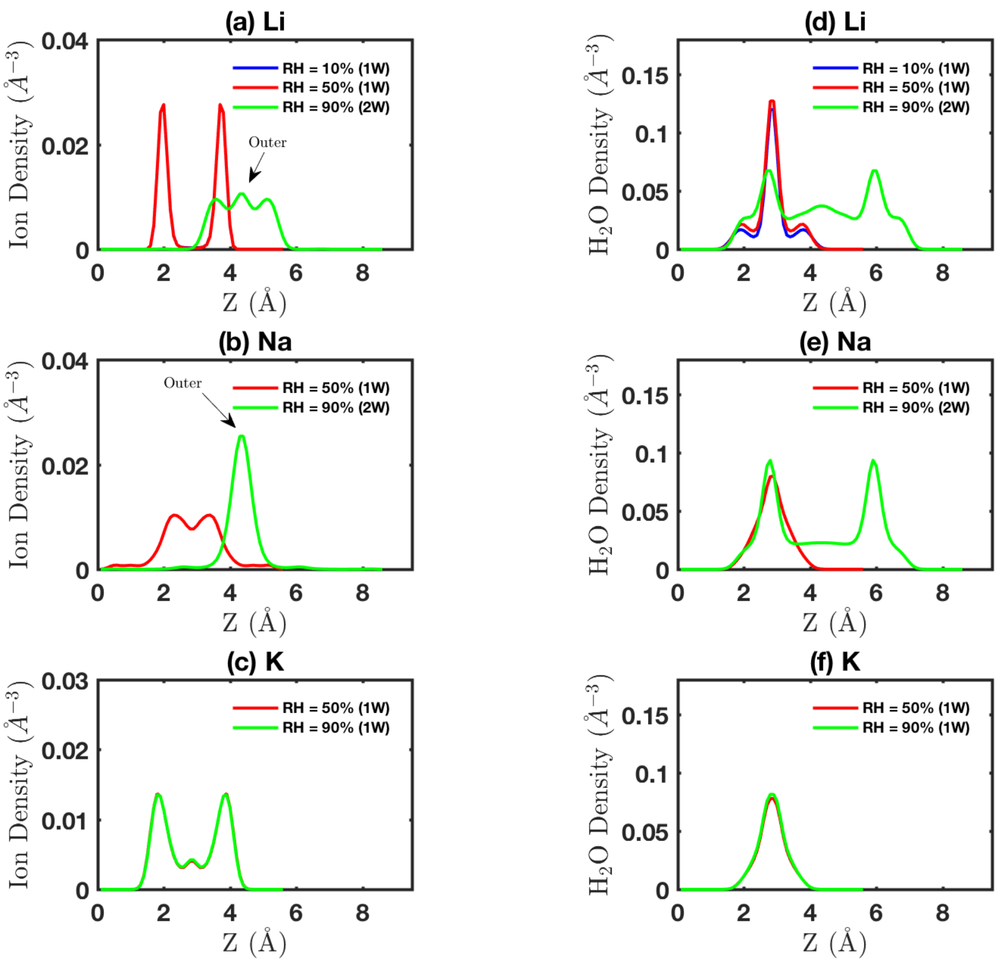

Figure S3: Equilibrium distributions of ions (left panels) and water molecules (right panels) in the interlayers of Arizona Li- (top panels), Na- (middle panels), and K-montmorillonite (bottom panels) at 298.15 K. Each origin corresponds to the clay surface oxygen (clay surface oxygen is also positioned at $z = d - 6.56$ Å). The arrows show outer-sphere ions. The basal $d-$spacings are as given in Table 2. (a,d) Li-, (b,e) Na-, and (c,f) K-montmorillonite.

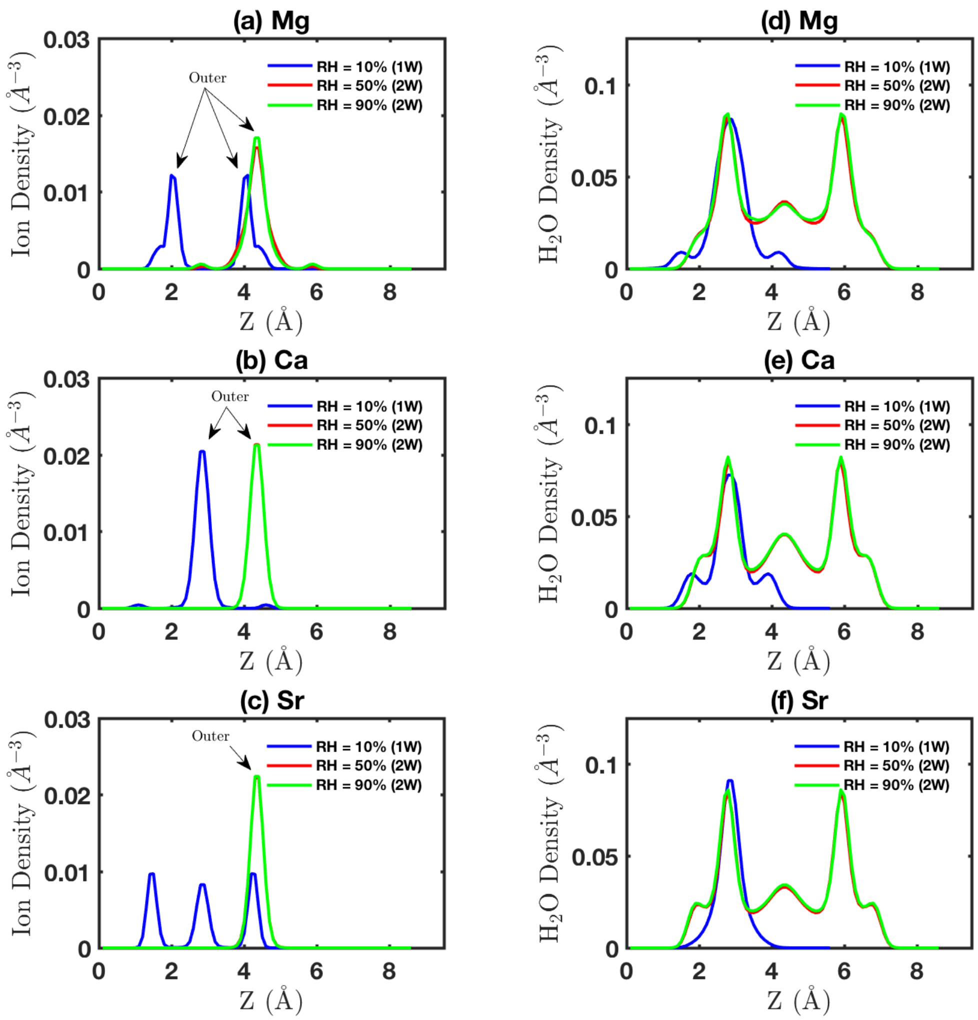

Figure S4: Same as in Fig. S3, but for Arizona Mg- (top panels), Ca- (middle panels), and Sr-montmorillonite (bottom panels). (a,d) Mg-, (b,e) Ca-, and (c,f) Sr-montmorillonite.

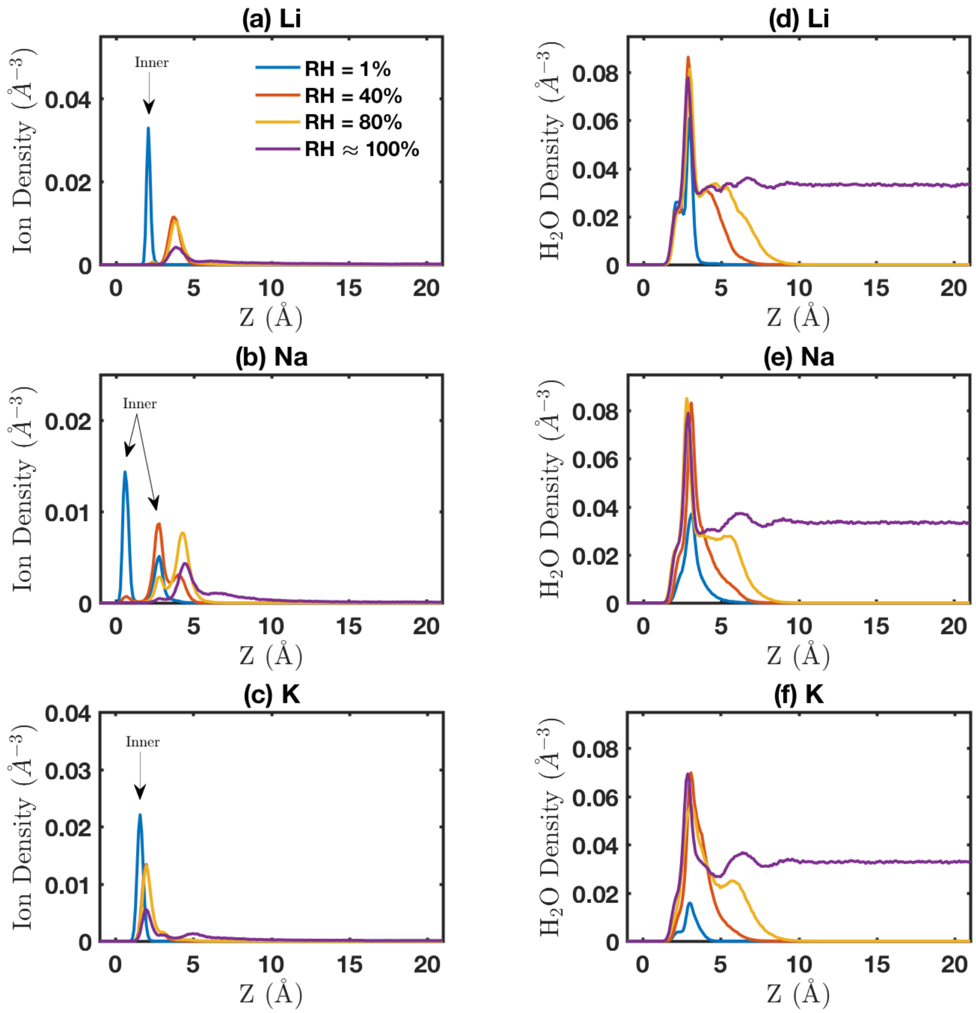

Figure S5: Equilibrium distributions of ions (left panels) and water molecules (right panels) in the mesopores of Arizona Li- (top panels), Na- (middle panels), and K-montmorillonite (bottom panels) at 298.15 K. Each origin corresponds to the clay surface oxygen. The arrows show inner-sphere ions. The basal $d-$spacing is fixed at 65 Å. (a,d) Li-, (b,e) Na-, and (c,f) K-montmorillonite.

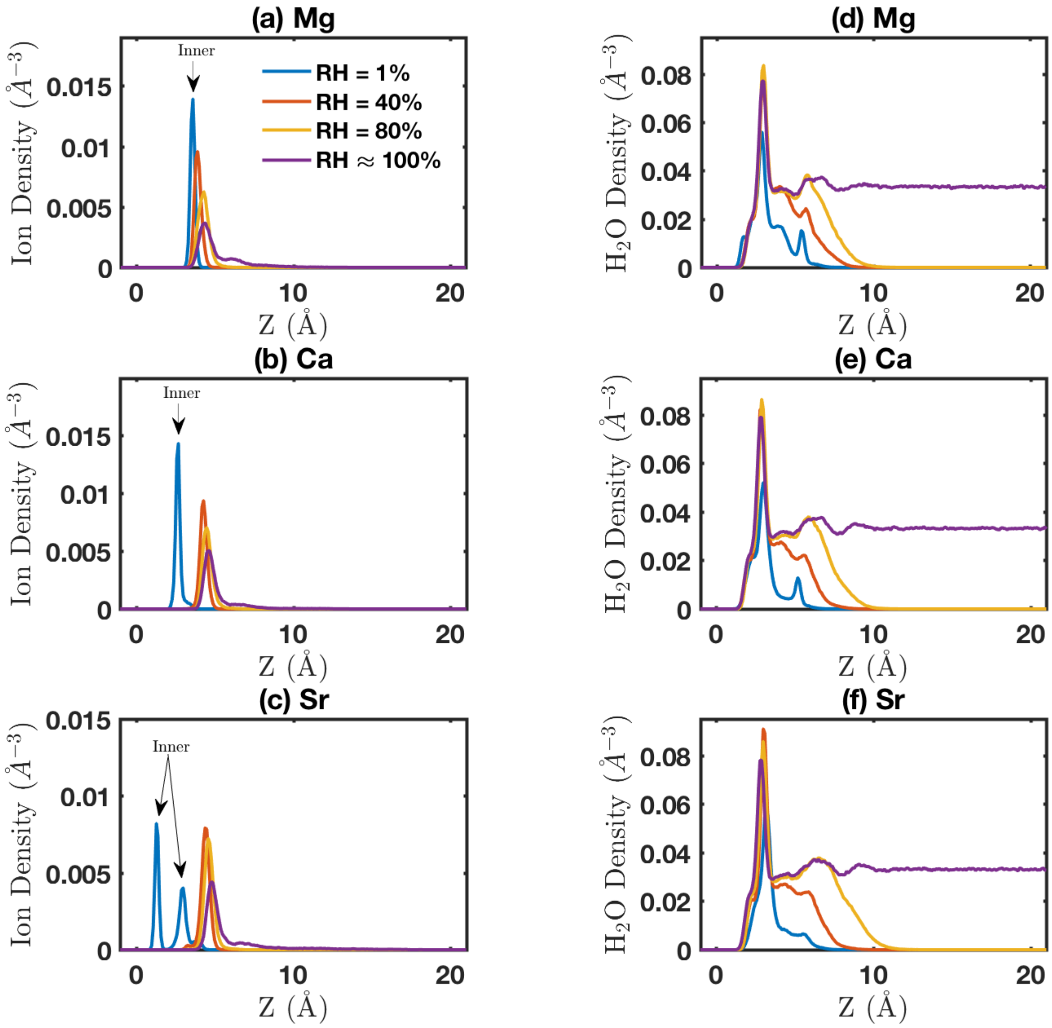

Figure S6: Same as in Fig. S5, but for Arizona Mg- (top panels), Ca- (middle panels), and Sr-montmorillonite (bottom panels). (a,d) Mg-, (b,e) Ca-, and (c,f) Sr-montmorillonite.

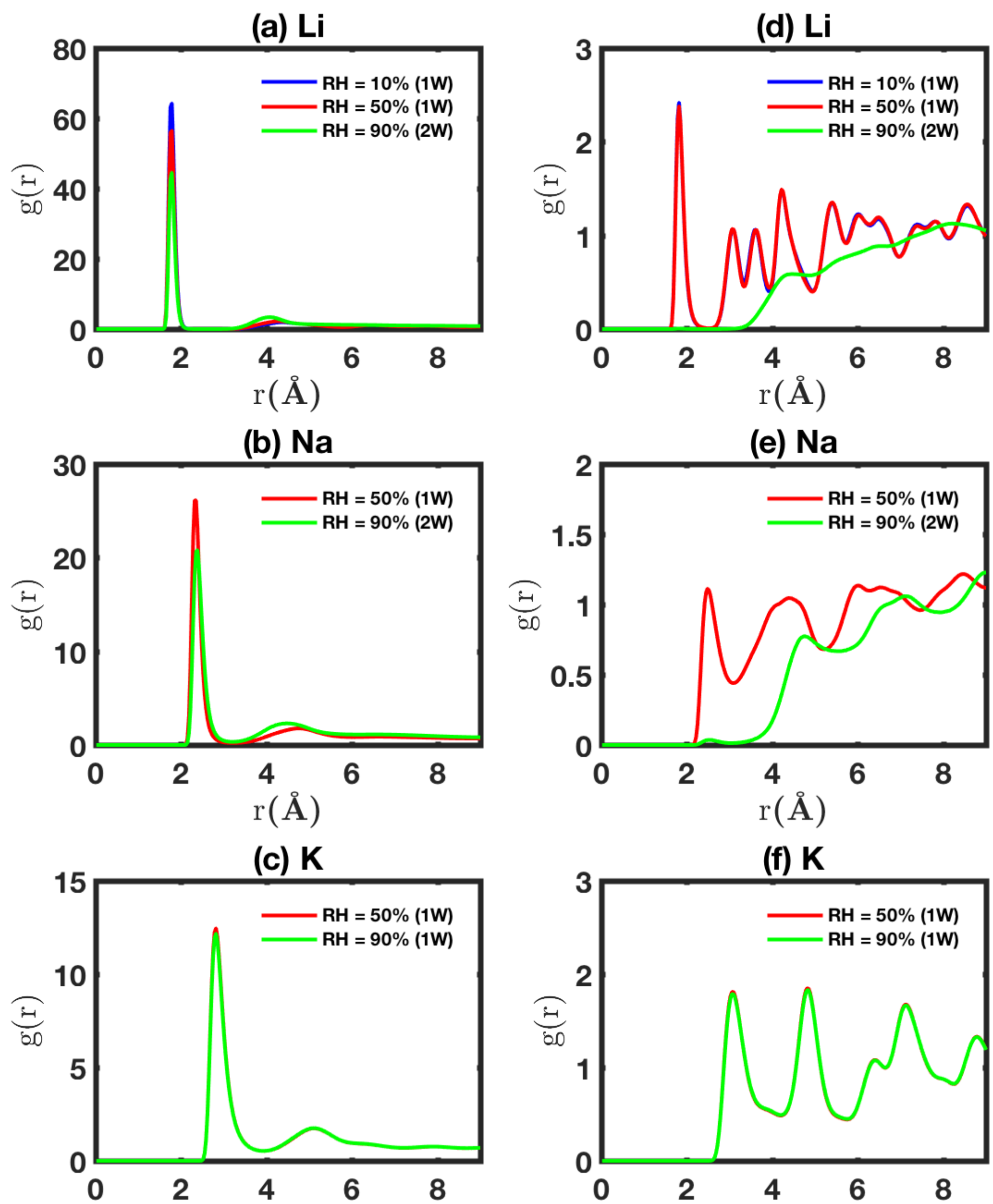

Figure S7: RDFs of ion-water oxygen (left panels) and ion-clay oxygen (right panels) for Arizona Li- (top panels), Na- (middle panels), and K-montmorillonite (bottom panels) at 298.15 K. The basal $d-$spacings are as given in Table 2. (a,d) Li-, (b,e) Na-, and (c,f) K-montmorillonite.

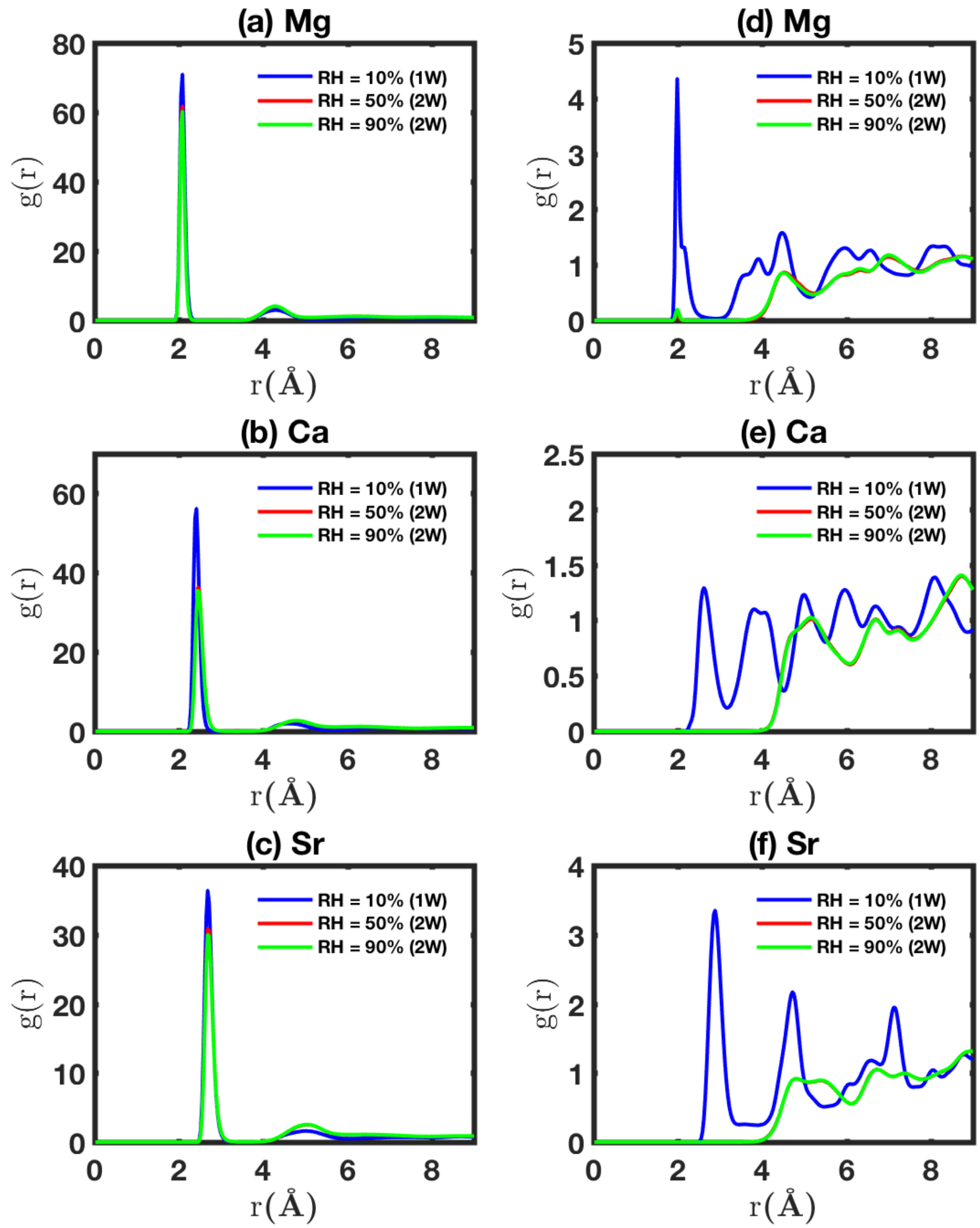

Figure S8: Same as in Fig. S7, but for Arizona Mg- (top panels), Ca- (middle panels), and Sr-montmorillonite (bottom panels). (a,d) Mg-, (b,e) Ca-, and (c,f) Sr-montmorillonite.

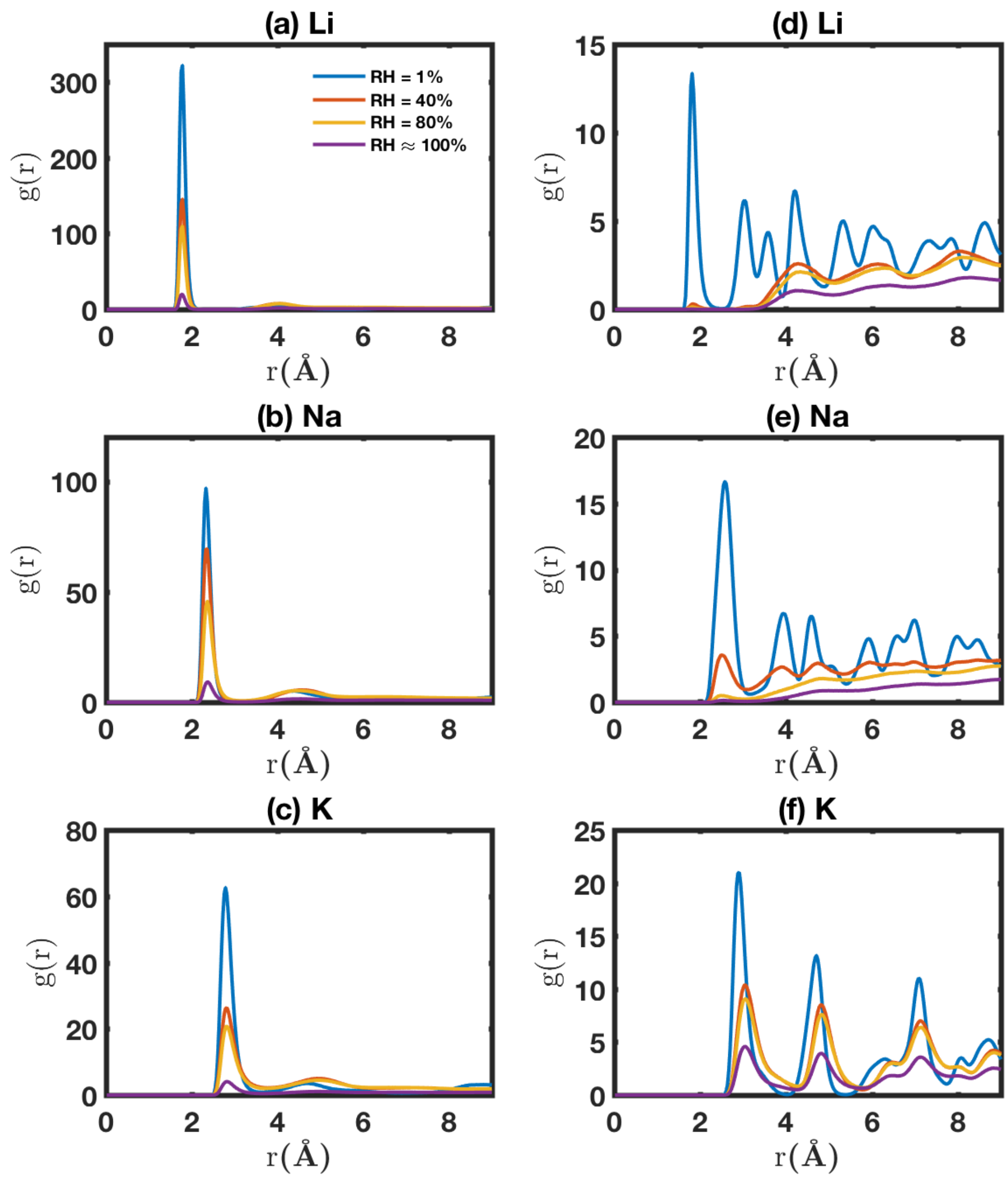

Figure S9: RDFs of ion-water oxygen (left panels) and ion-clay oxygen (right panels) for Arizona Li- (top panels), Na- (middle panels), and K-montmorillonite (bottom panels) at 298.15 K. The basal $d-$spacing is fixed at 65 Å. (a,d) Li-, (b,e) Na-, and (c,f) K-montmorillonite.

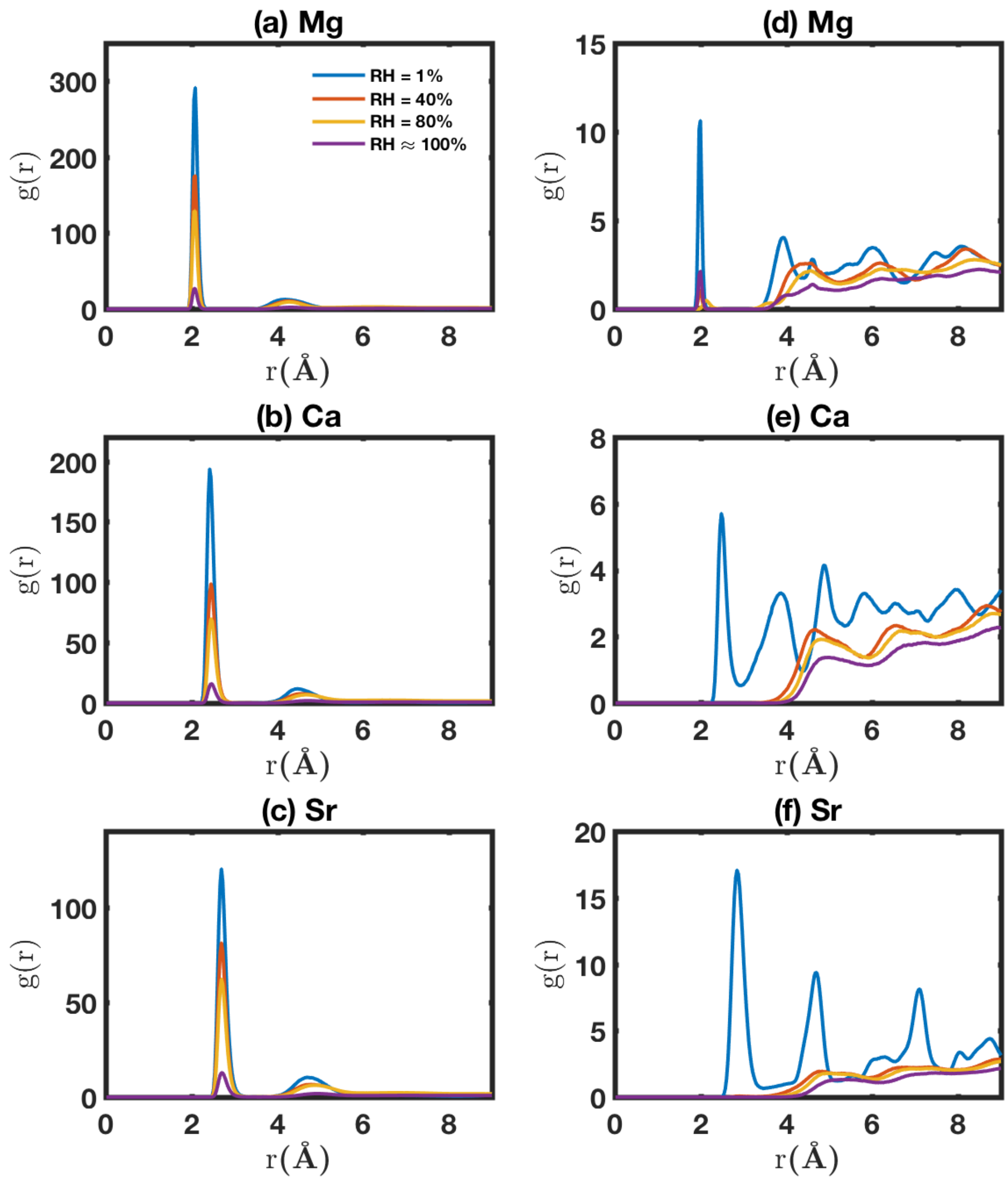

Figure S10: Same as in Fig. S9, but for Arizona Mg- (top panels), Ca- (middle panels), and Sr-montmorillonite (bottom panels). (a,d) Mg-, (b,e) Ca-, and (c,f) Sr-montmorillonite.

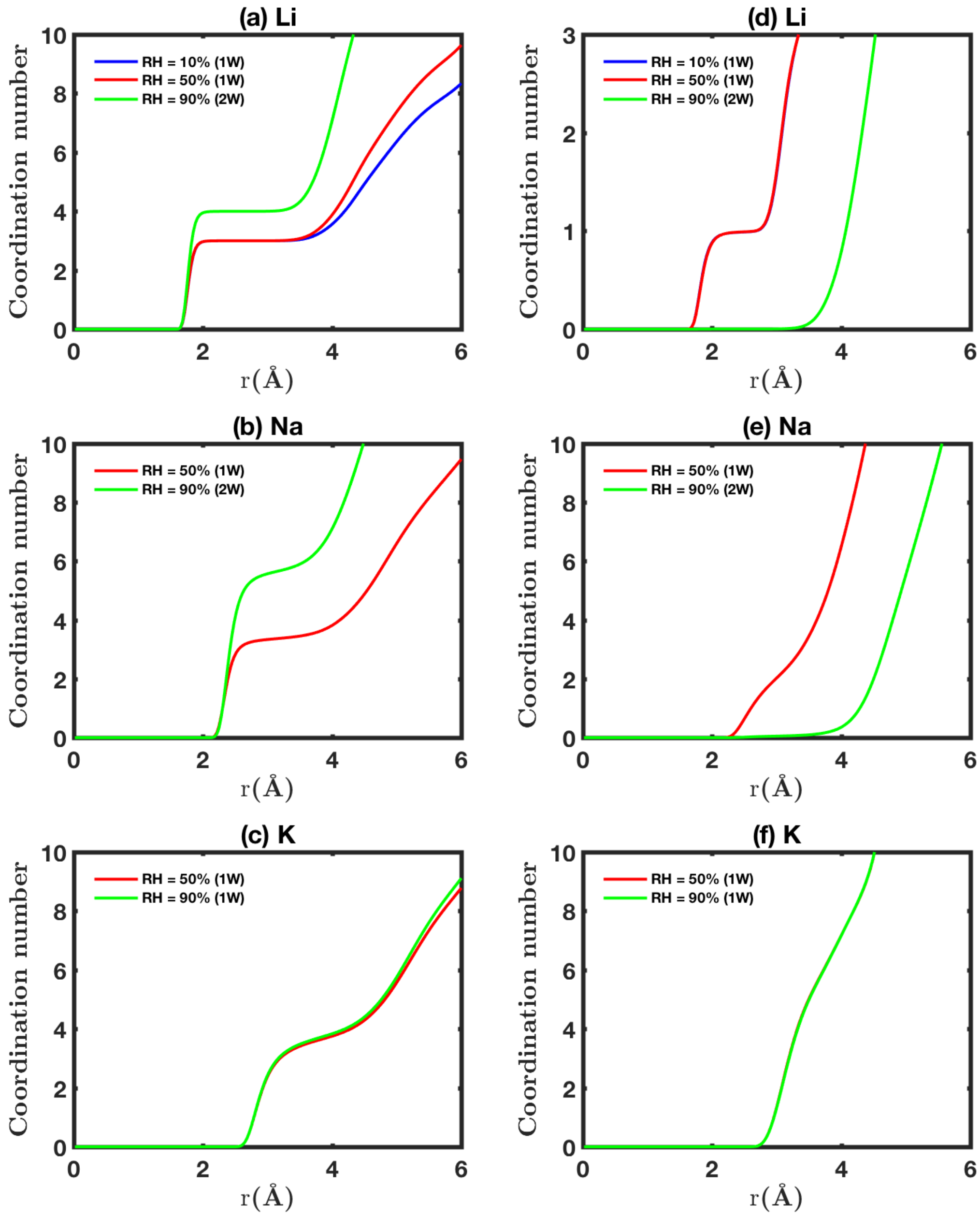

Figure S11: The running coordination numbers obtained by integrating $g(r)$ from 0 to r of ion-water oxygen (left panels) and ion-clay oxygen (right panels) for Arizona Li- (top panels), Na- (middle panels), and K-montmorillonite (bottom panels) at 298.15 K. The basal $d-$spacings are as given in Table 2. (a,d) Li-, (b,e) Na-, and (c,f) K-montmorillonite.

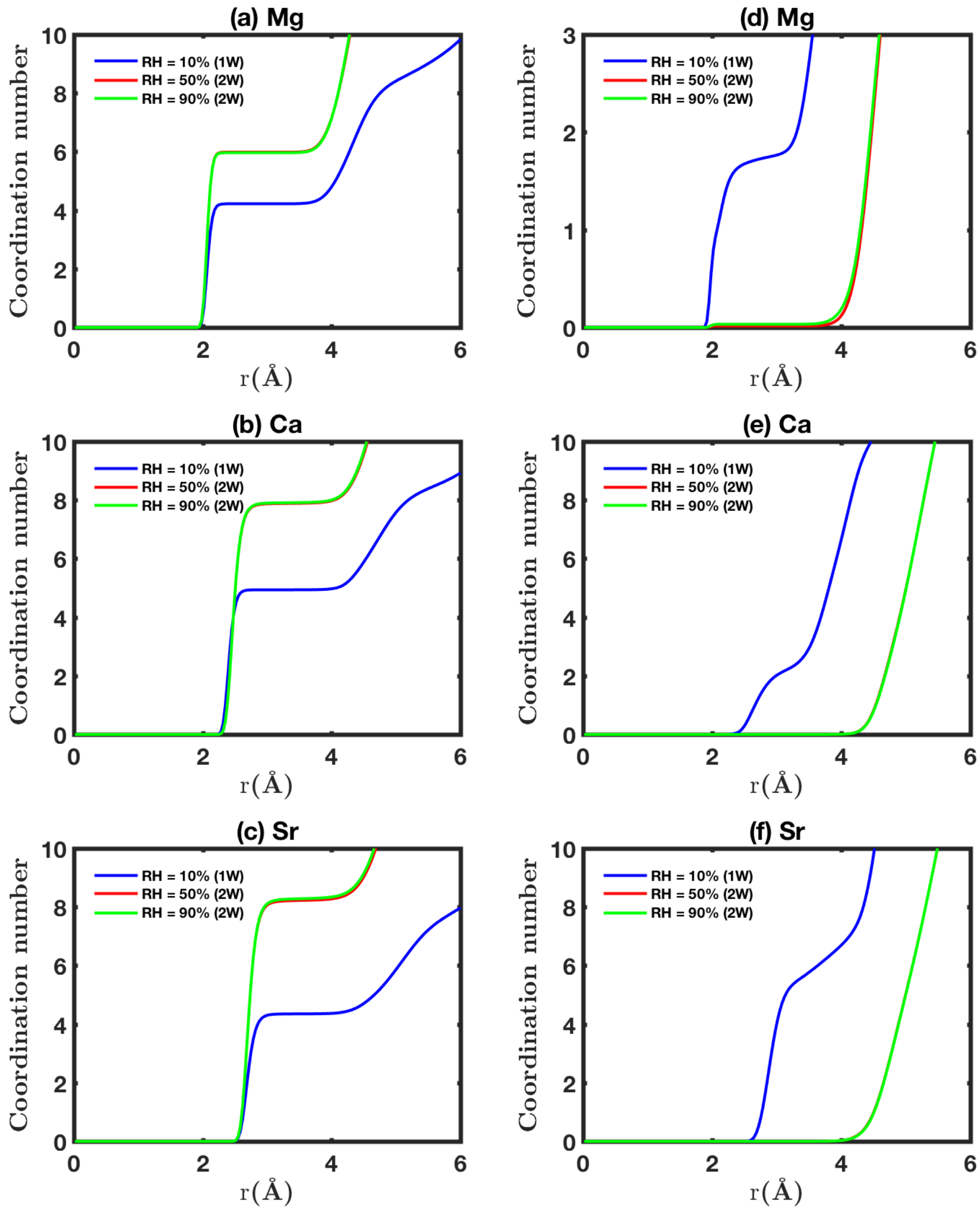

Figure S12: Same as in Fig. S11, but for Arizona Mg- (top panels), Ca- (middle panels), and Sr-montmorillonite (bottom panels). (a,d) Mg-, (b,e) Ca-, and (c,f) Sr-montmorillonite.

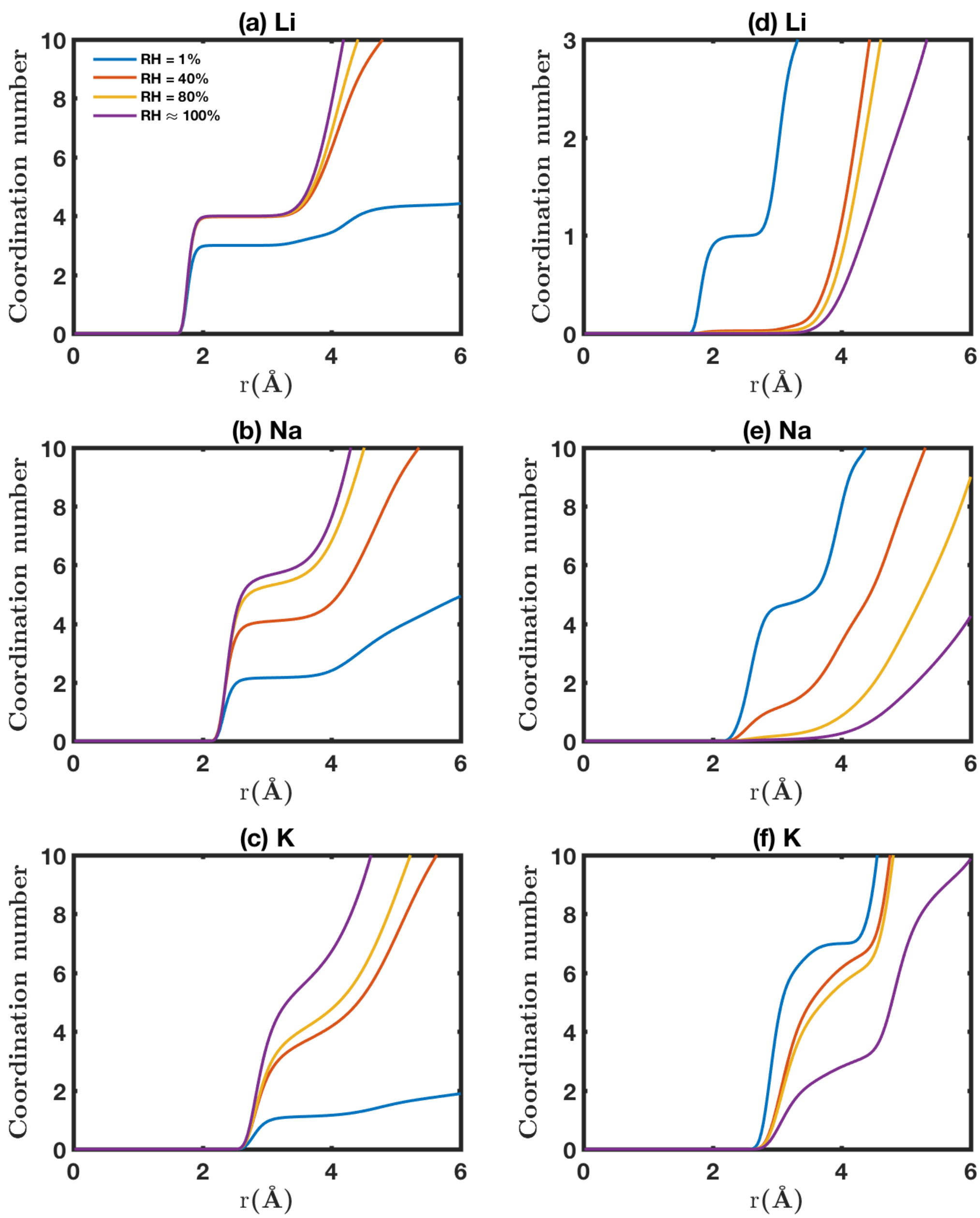

Figure S13: The running coordination numbers obtained by integrating $g(r)$ from 0 to r of ion-water oxygen (left panels) and ion-clay oxygen (right panels) for Arizona Li- (top panels), Na- (middle panels), and K-montmorillonite (bottom panels) at 298.15 K. The basal $d-$spacing is fixed at 65 Å. (a,d) Li-, (b,e) Na-, and (c,f) K-montmorillonite.

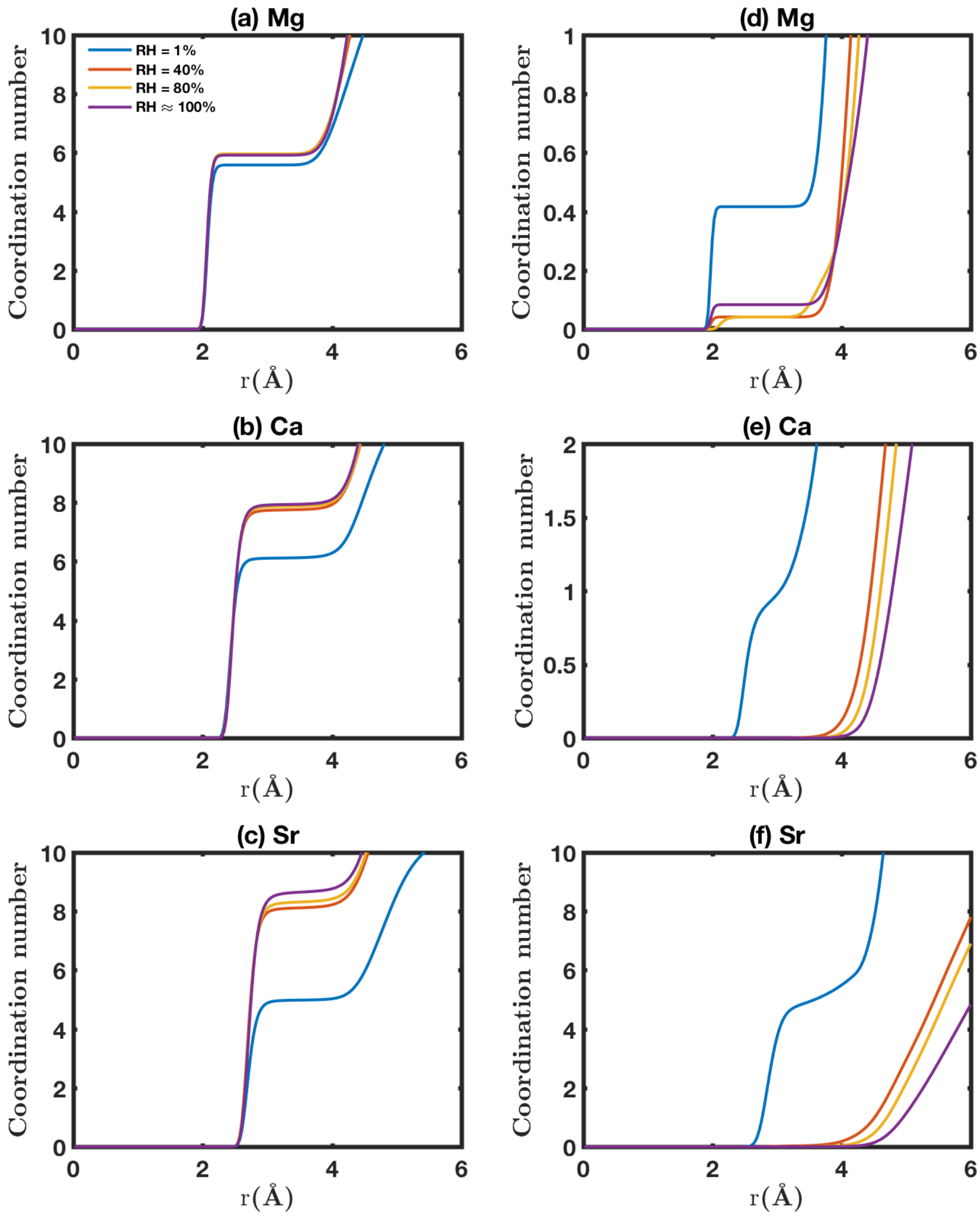

Figure S14: Same as in Fig. S13, but for Arizona Mg- (top panels), Ca- (middle panels), and Sr-montmorillonite (bottom panels). (a,d) Mg-, (b,e) Ca-, and (c,f) Sr-montmorillonite.

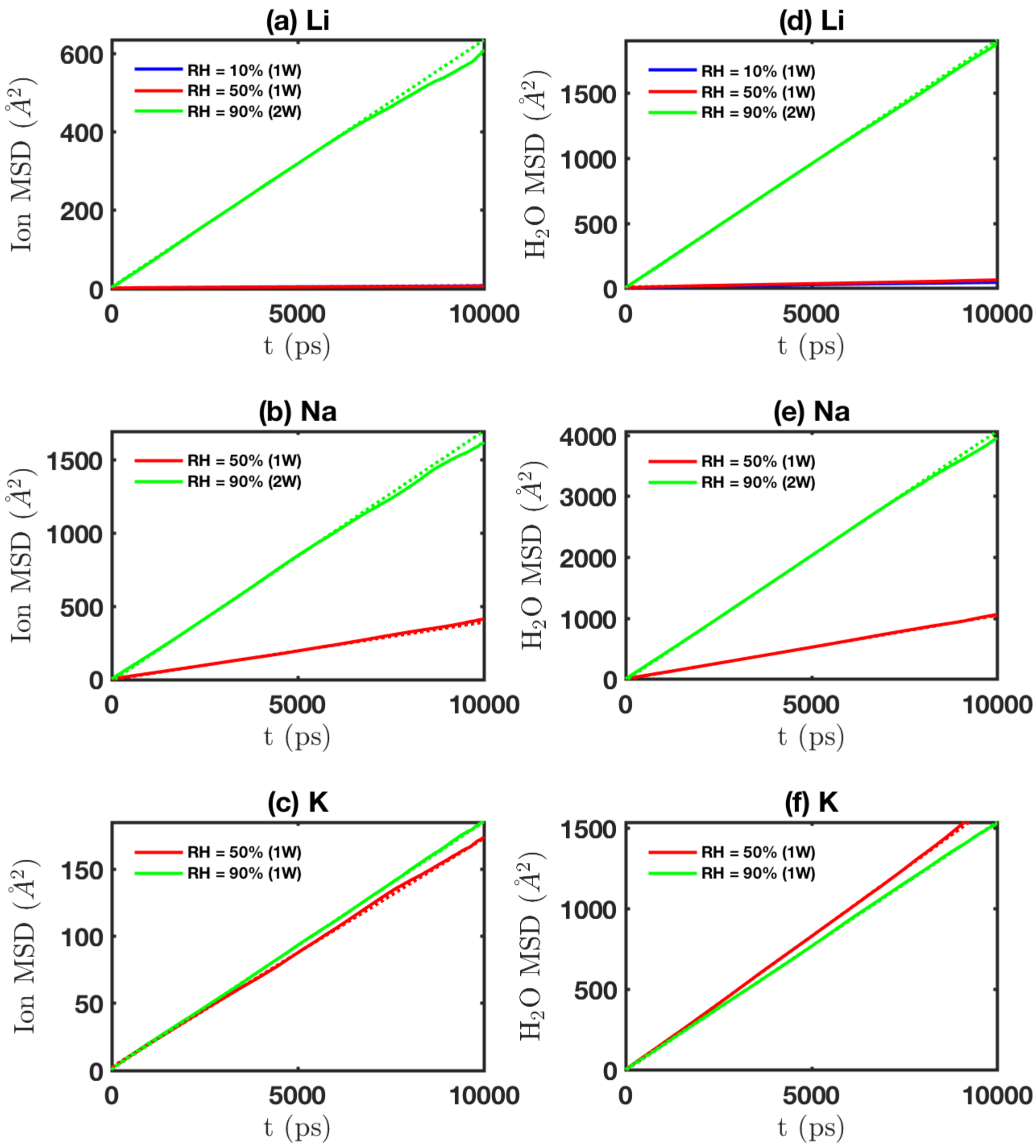

Figure S15: MSDs in the xy plane (parallel to the surfaces) of ions (left panels) and water molecules (right panels) in the interlayers of Arizona Li- (top panels), Na- (middle panels), and K-montmorillonite (bottom panels) at 298.15 K. The basal $d-$spacings are as given in Table 2. (a,d) Li-, (b,e) Na-, and (c,f) K-montmorillonite.

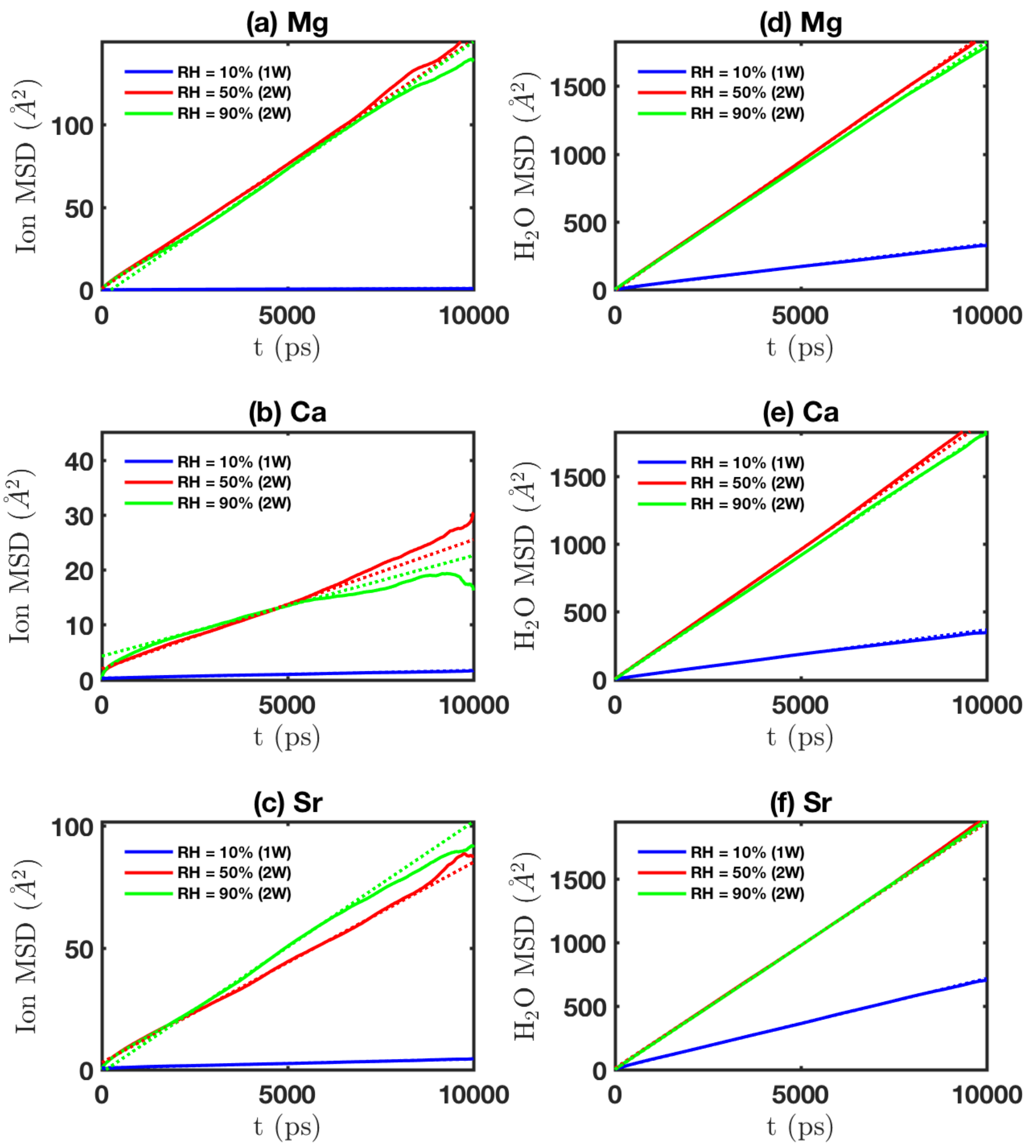

Figure S16: Same as in Fig. S15, but for Arizona Mg- (top panels), Ca- (middle panels), and Sr-montmorillonite (bottom panels). (a,d) Mg-, (b,e) Ca-, and (c,f) Sr-montmorillonite.

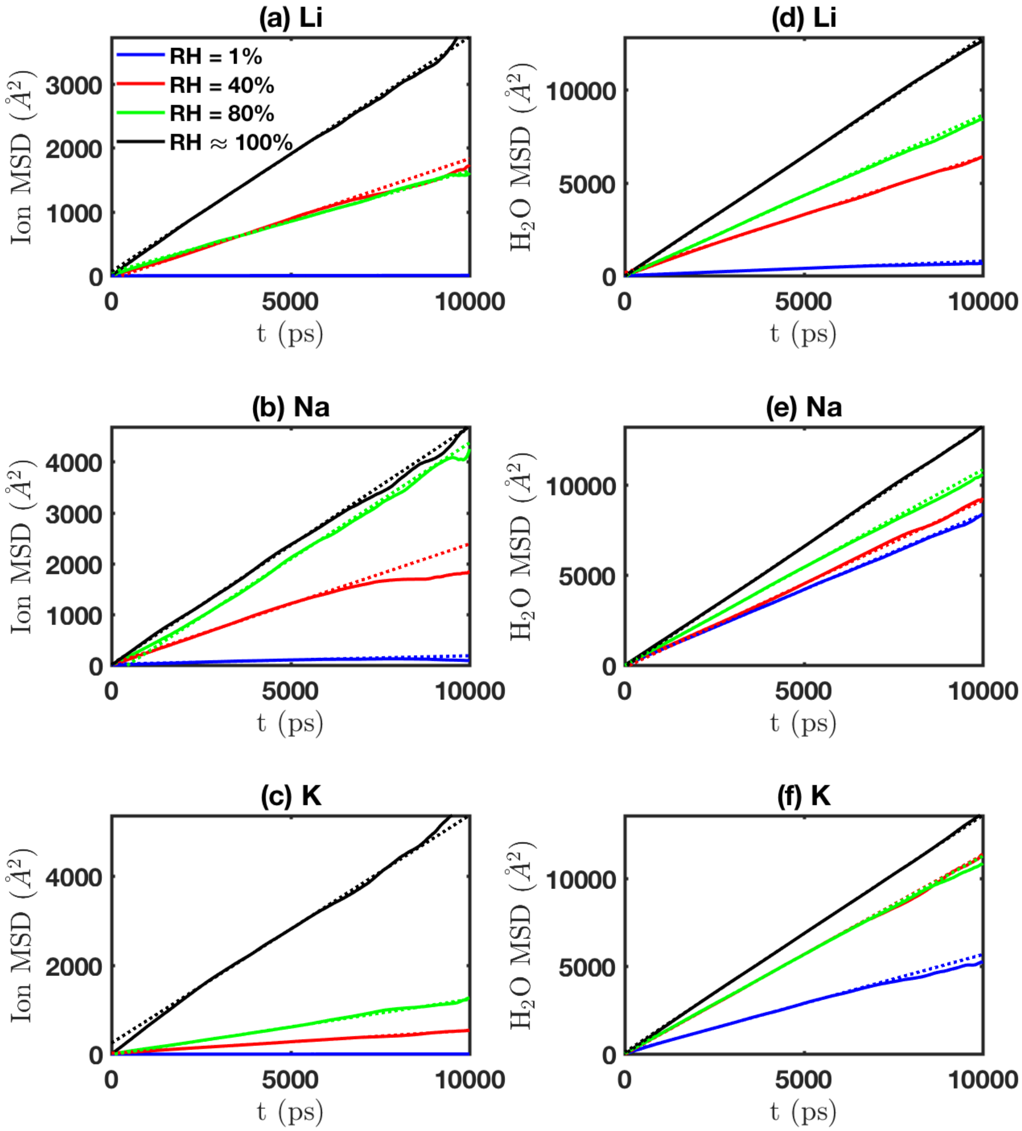

Figure S17: MSDs in the xy plane (parallel to the surfaces) of ions (left panels) and water molecules (right panels) in the mesopores of Arizona Li- (top panels), Na- (middle panels), and K-montmorillonite (bottom panels) at 298.15 K. The basal $d-$spacing is fixed at 65 Å. (a,d) Li-, (b,e) Na-, and (c,f) K-montmorillonite.

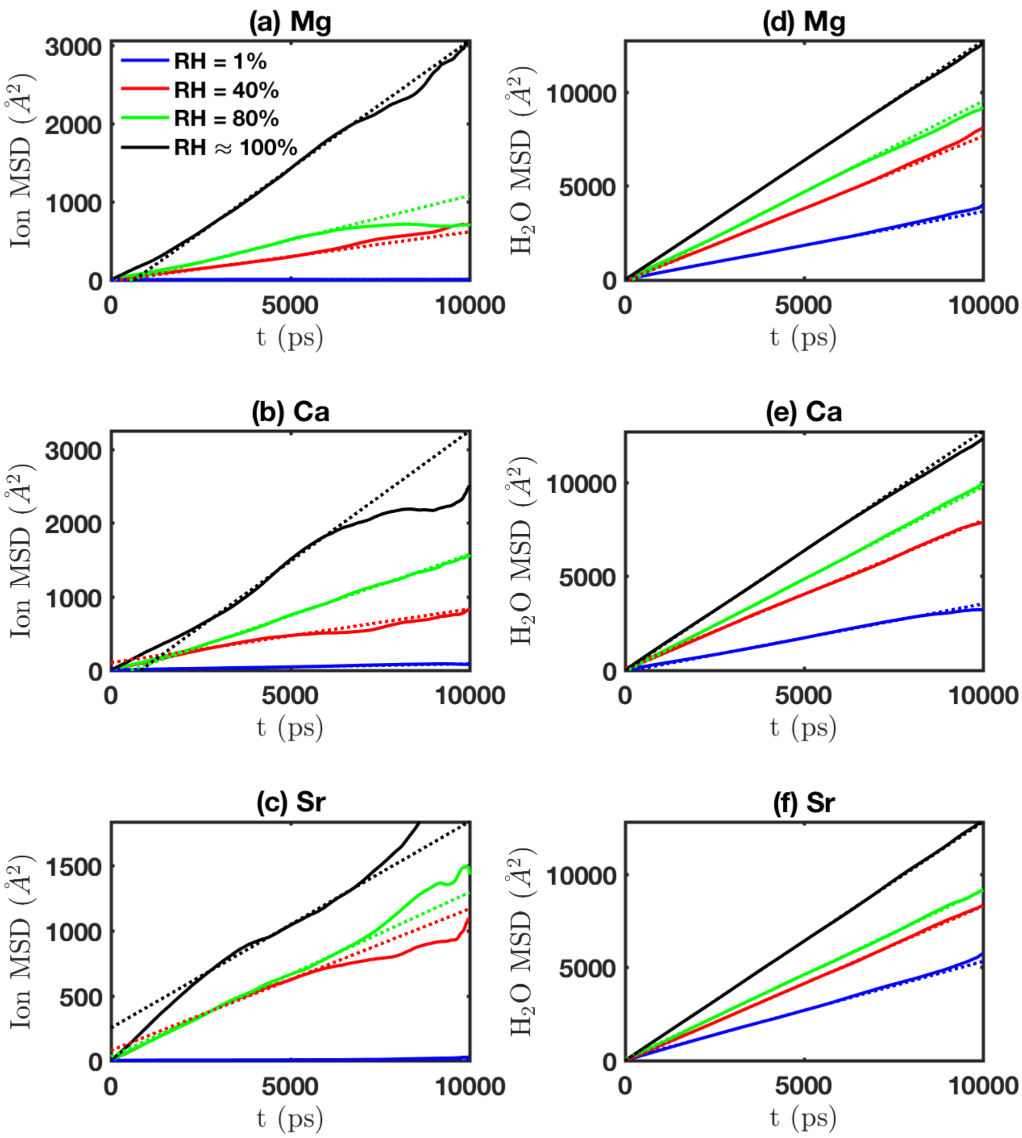

Figure S18: Same as in Fig. S17, but for Arizona Mg- (top panels), Ca- (middle panels), and Sr-montmorillonite (bottom panels). (a,d) Mg-, (b,e) Ca-, and (c,f) Sr-montmorillonite.

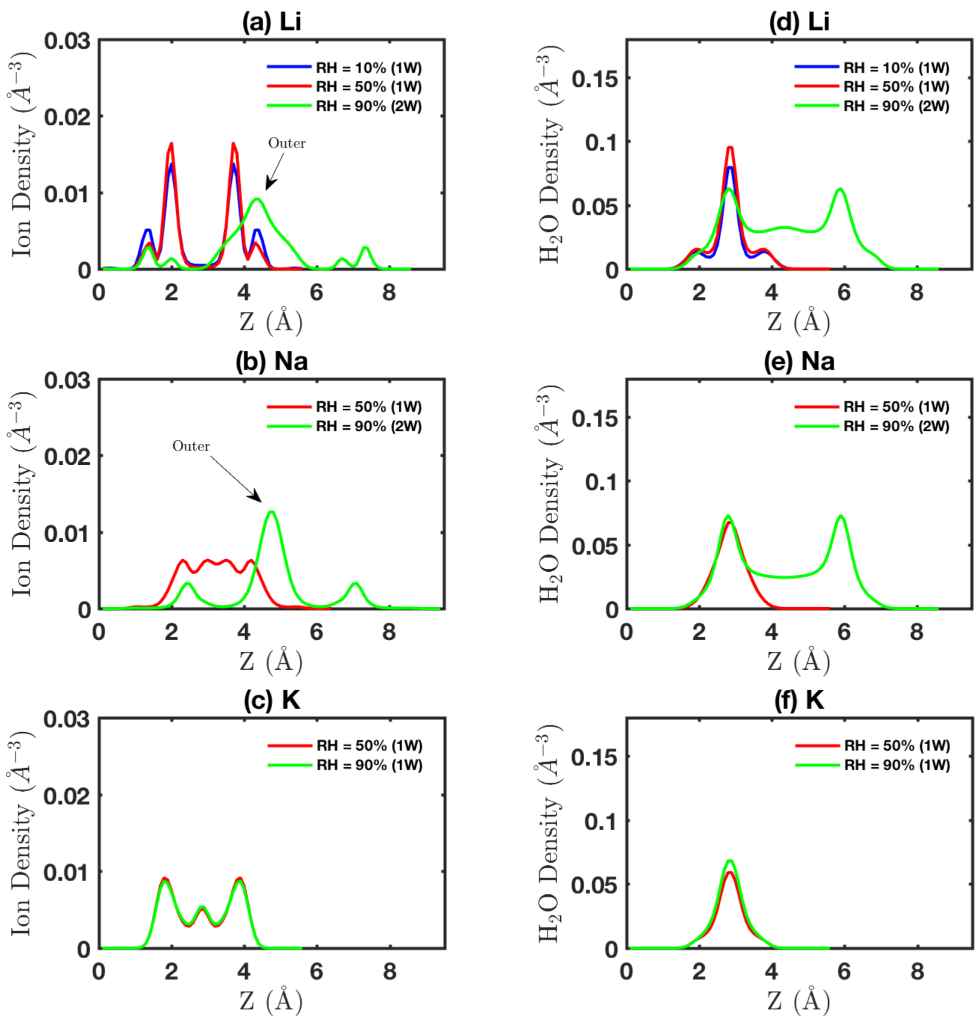

Figure S19: Same as in Fig. S3, but for Wyoming montmorillonite. The basal $d-$spacings are as given in Table S6.

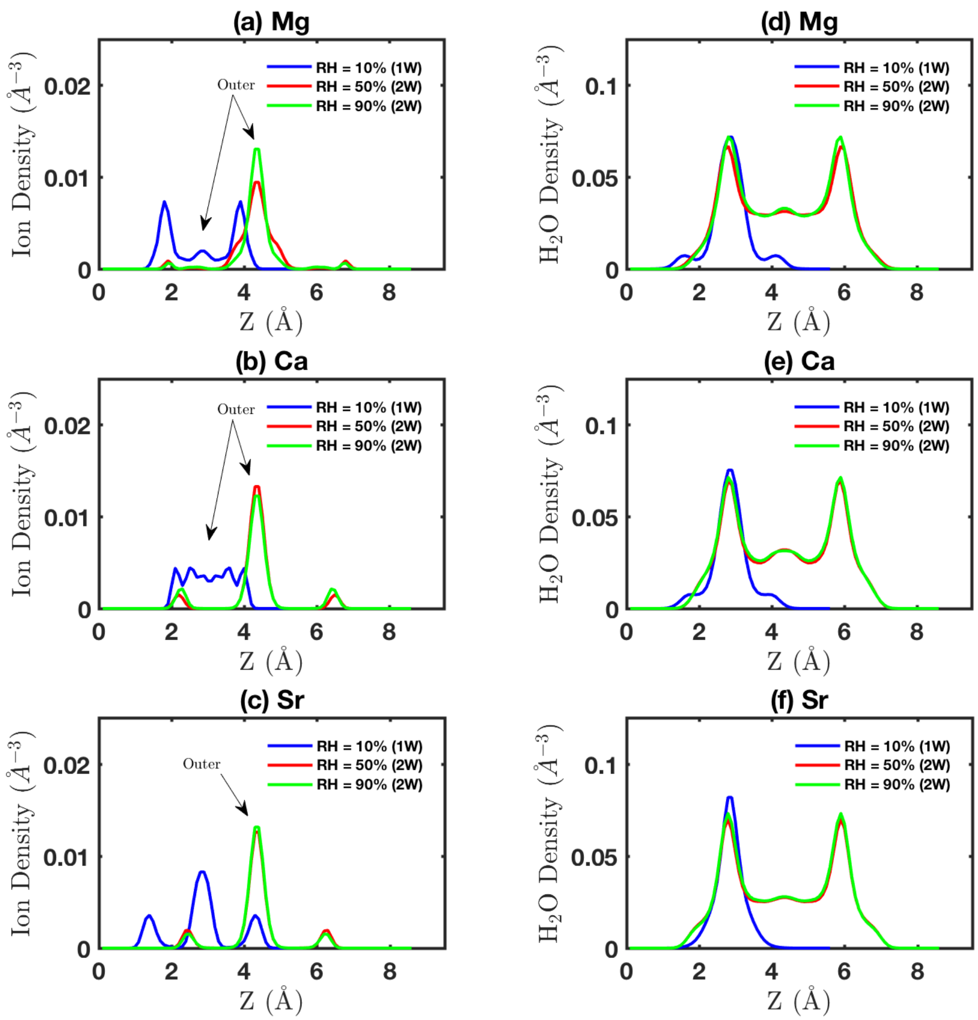

Figure S20: Same as in Fig. S4, but for Wyoming montmorillonite. The basal $d-$spacings are as given in Table S6.

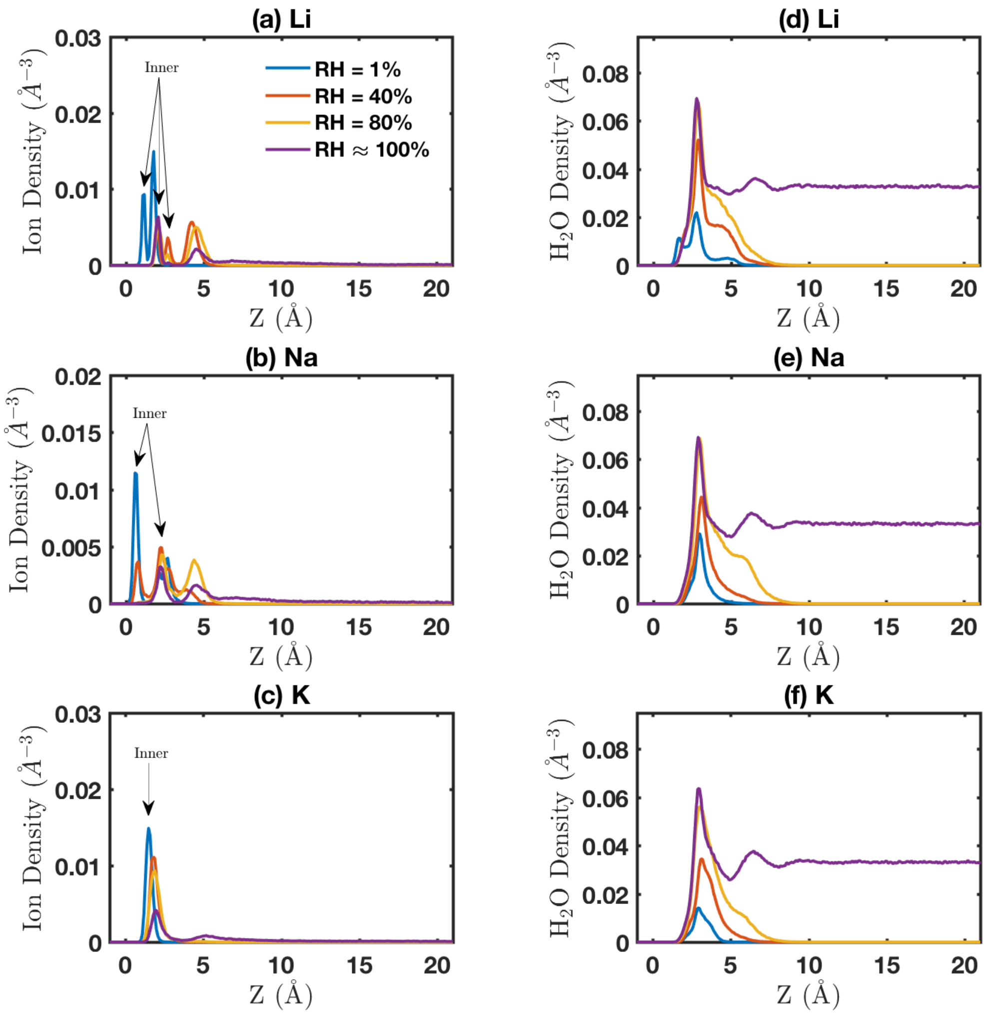

Figure S21: Same as in Fig. S5, but for Wyoming montmorillonite.

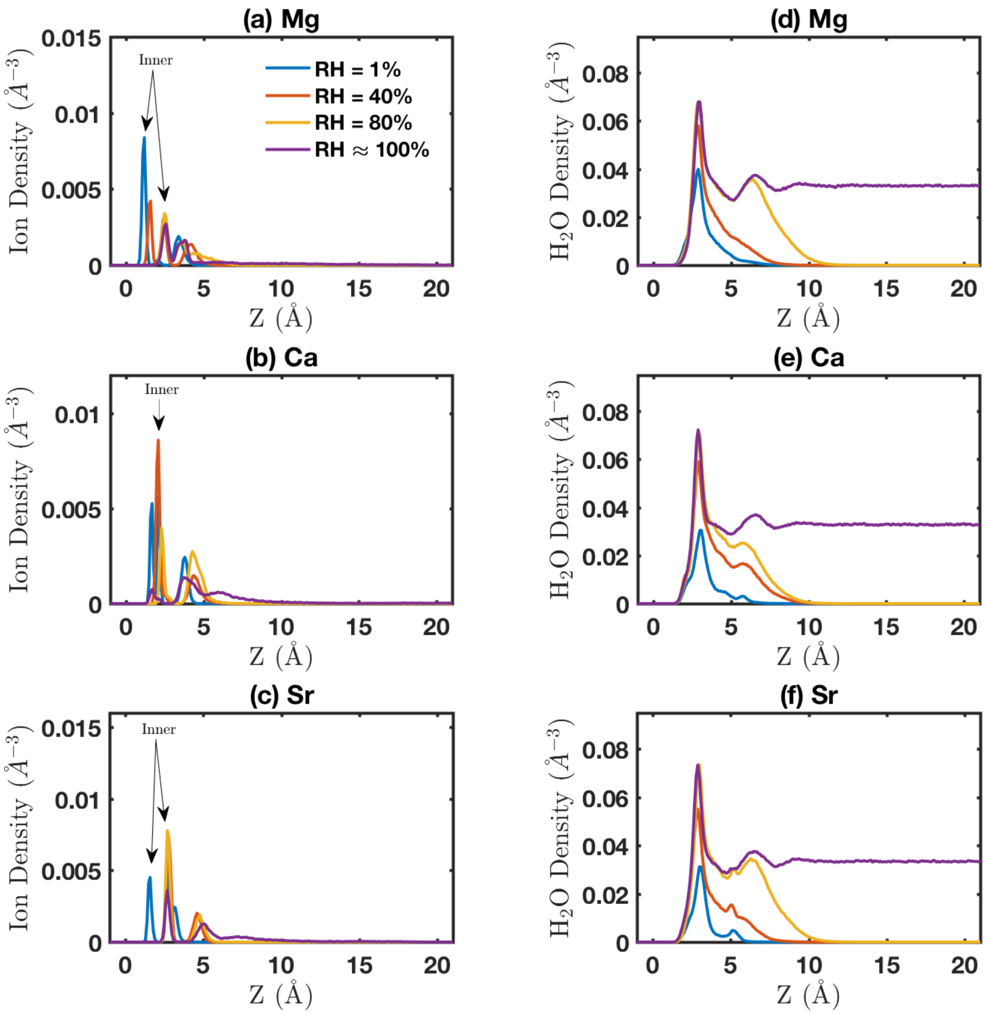

Figure S22: Same as in Fig. S6, but for Wyoming montmorillonite.

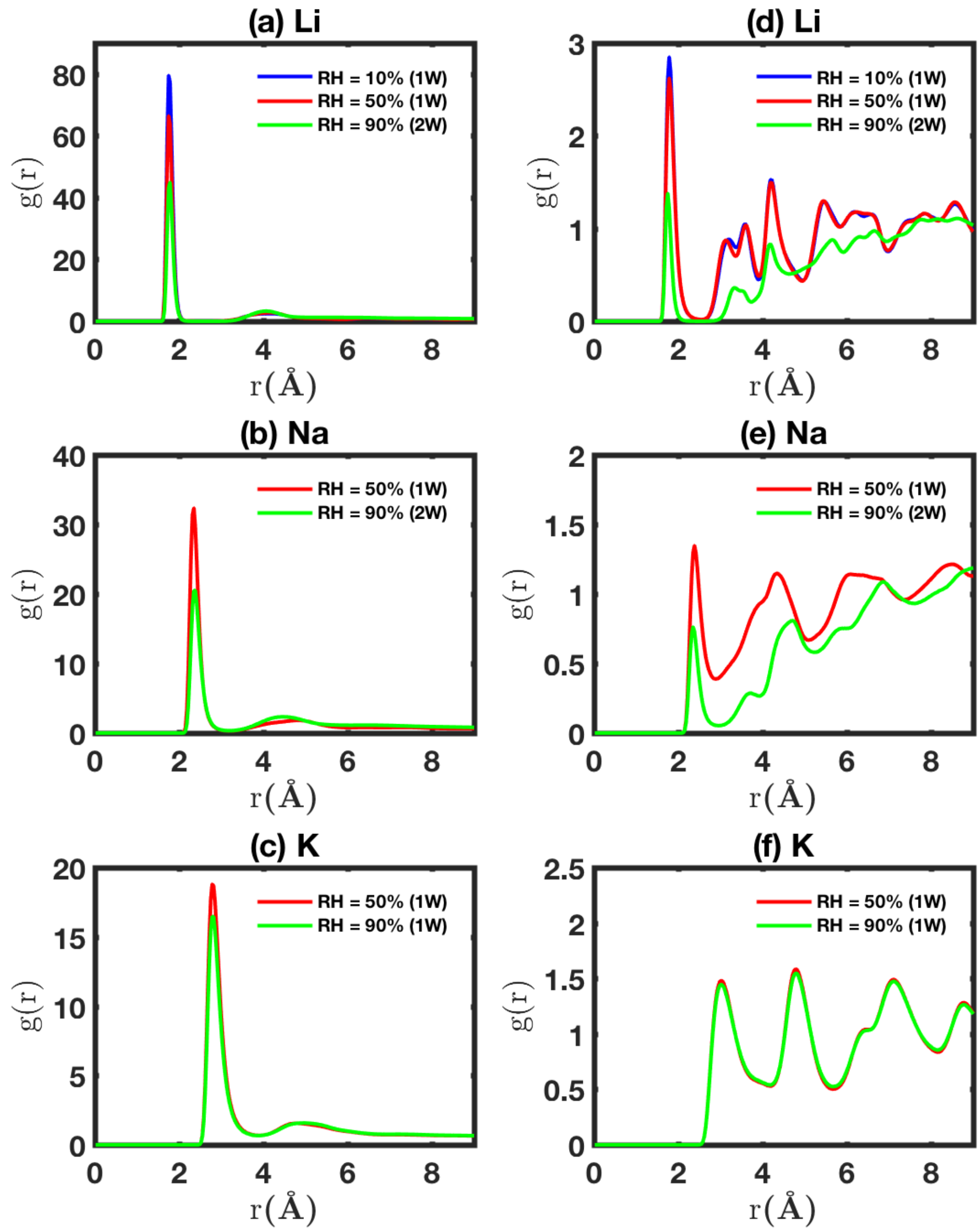

Figure S23: Same as in Fig. S7, but for Wyoming montmorillonite. The basal $d-$spacings are as given in Table S6.

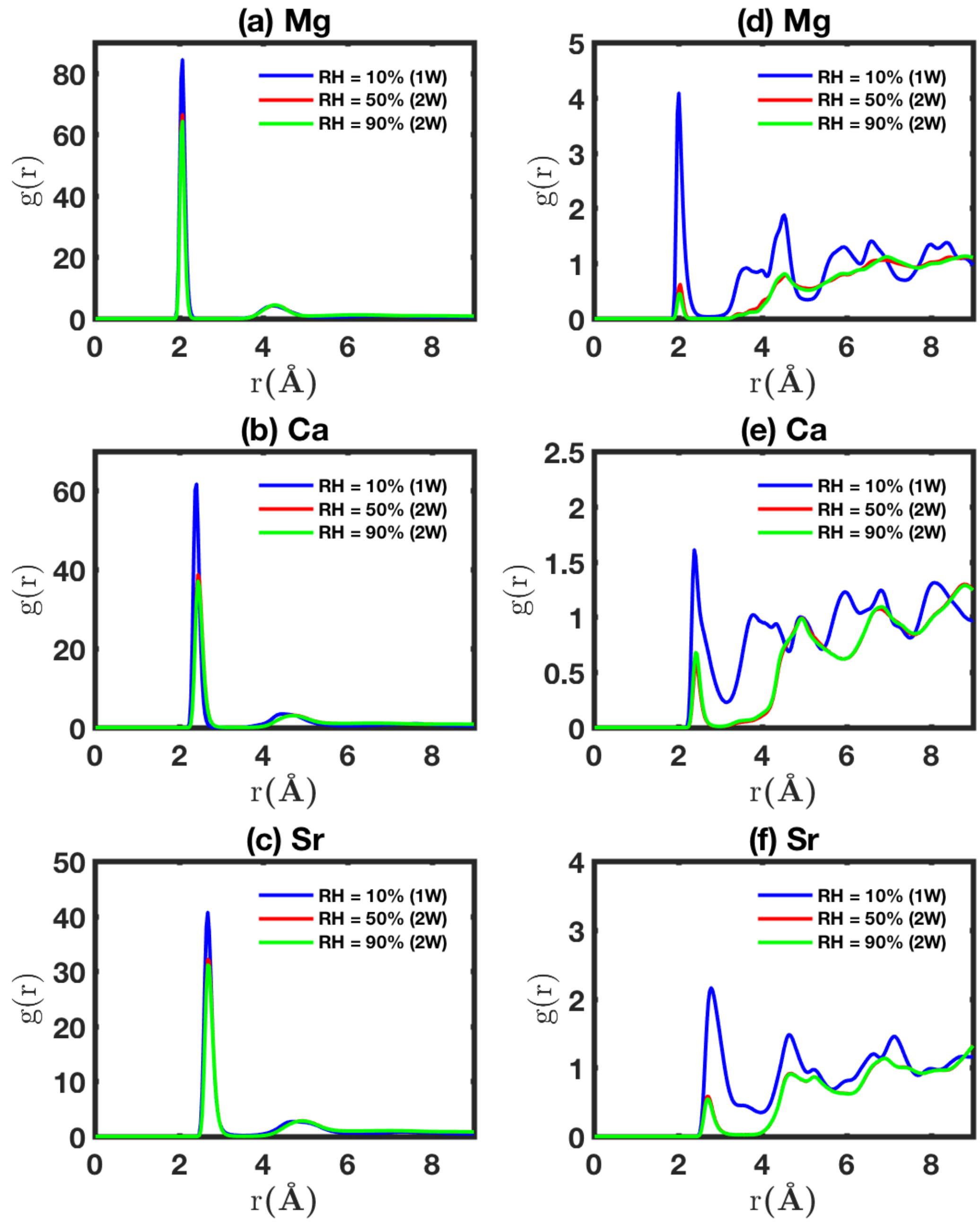

Figure S24: Same as in Fig. S8, but for Wyoming montmorillonite. The basal $d-$spacings are as given in Table S6.

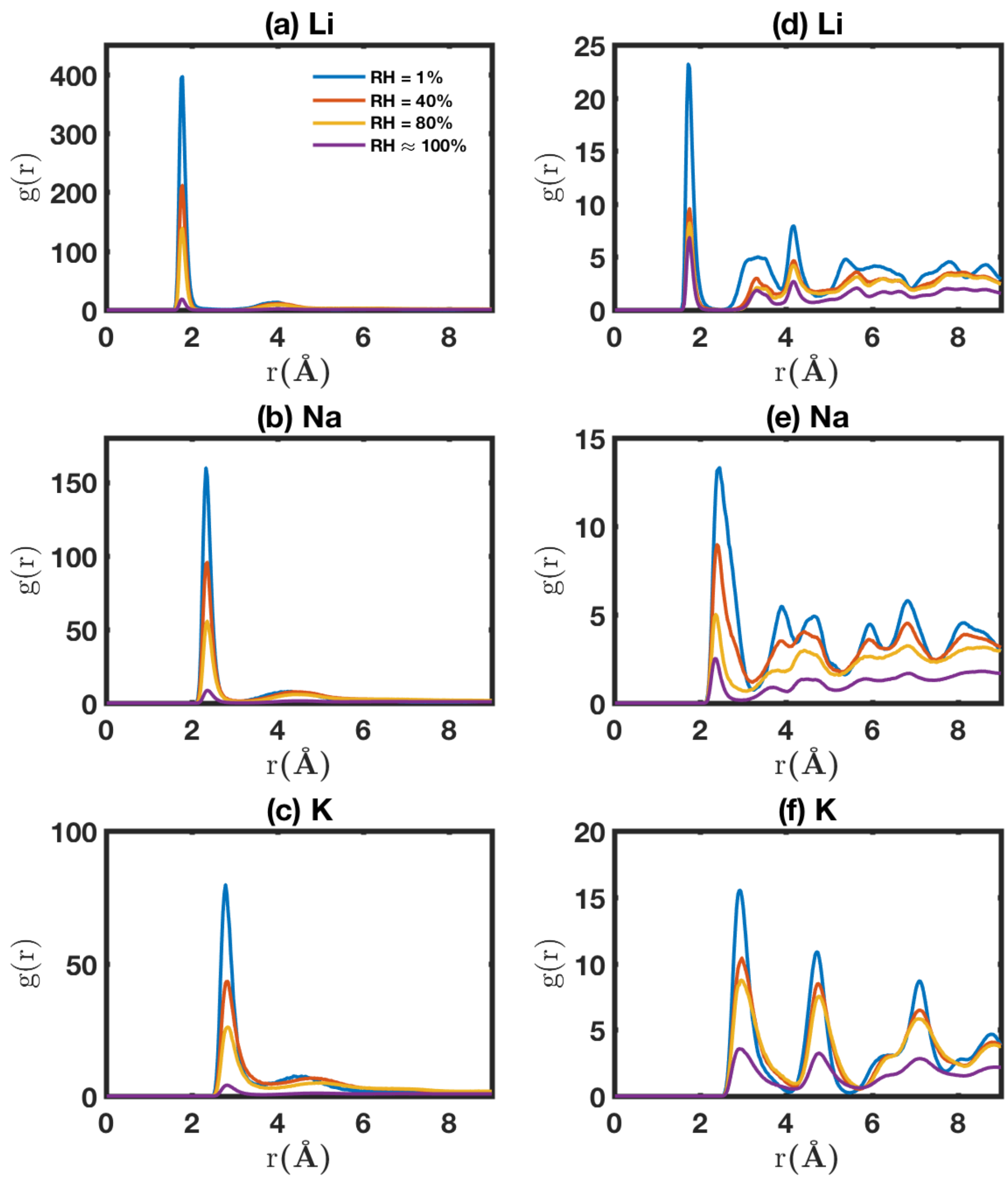

Figure S25: Same as in Fig. S9, but for Wyoming montmorillonite.

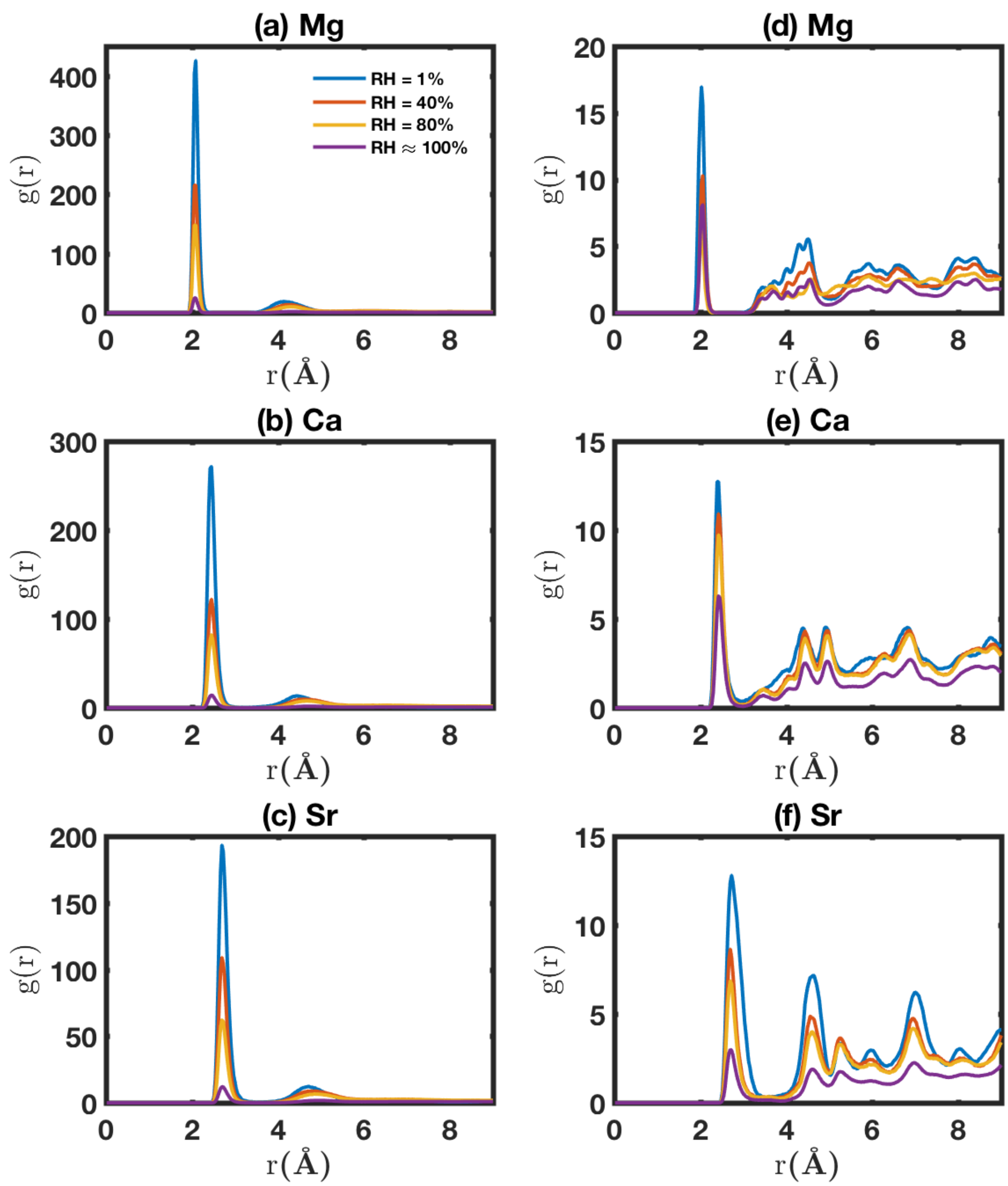

Figure S26: Same as in Fig. S10, but for Wyoming montmorillonite.

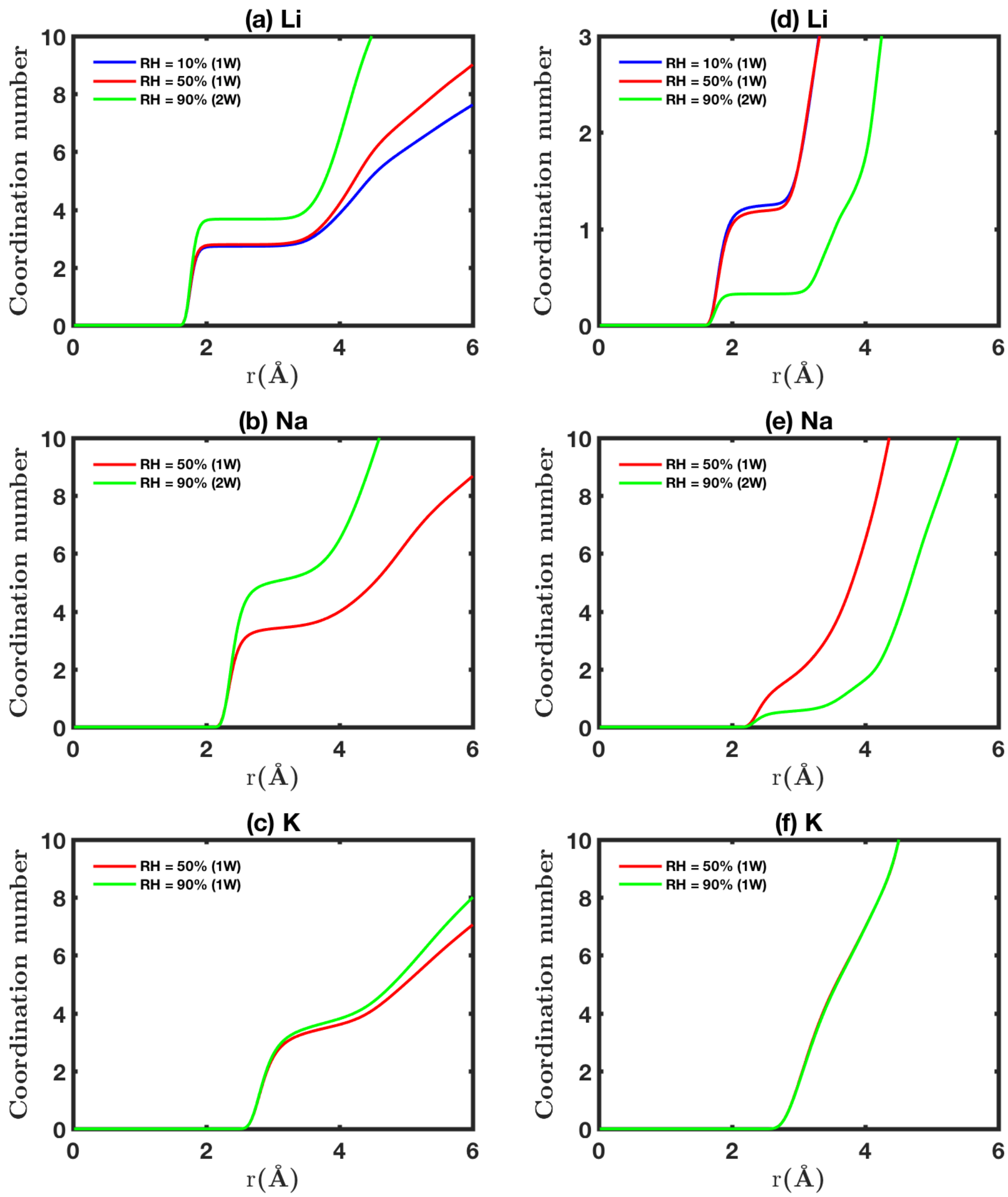

Figure S27: Same as in Fig. S11, but for Wyoming montmorillonite. The basal d−spacings are as given in Table S6.

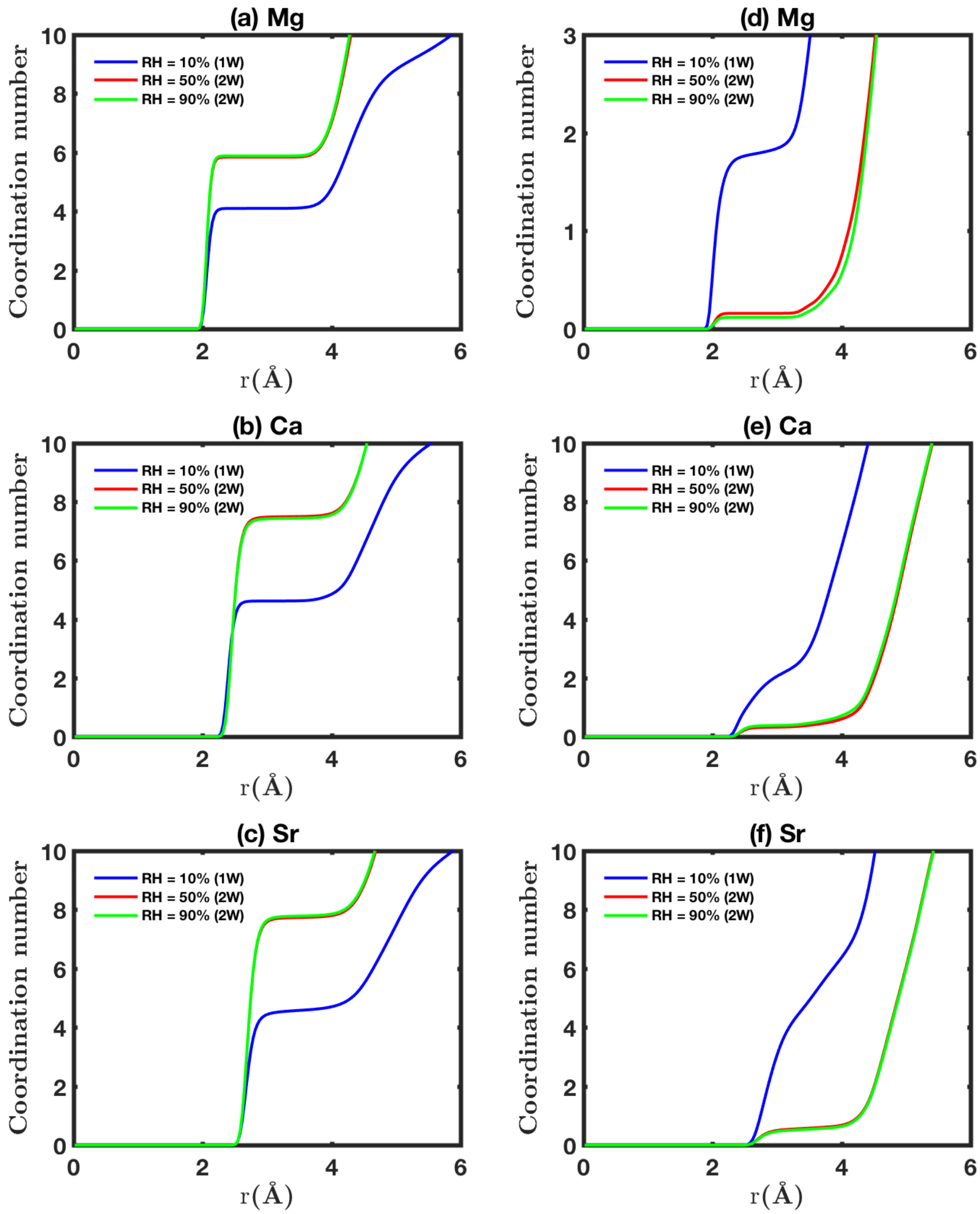

Figure S28: Same as in Fig. S12, but for Wyoming montmorillonite. The basal $d-$spacings are as given in Table S6.

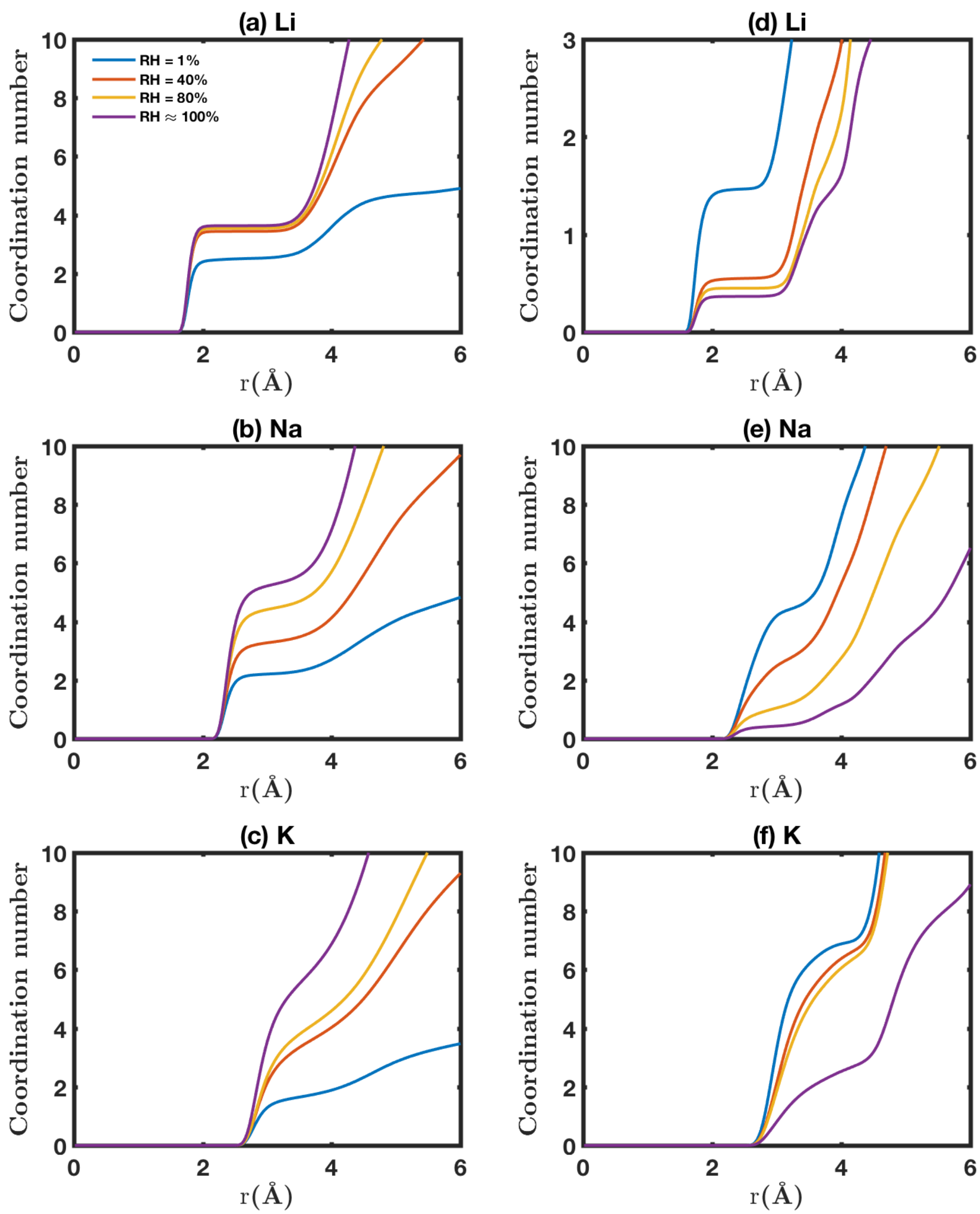

Figure S29: Same as in Fig. S13, but for Wyoming montmorillonite.

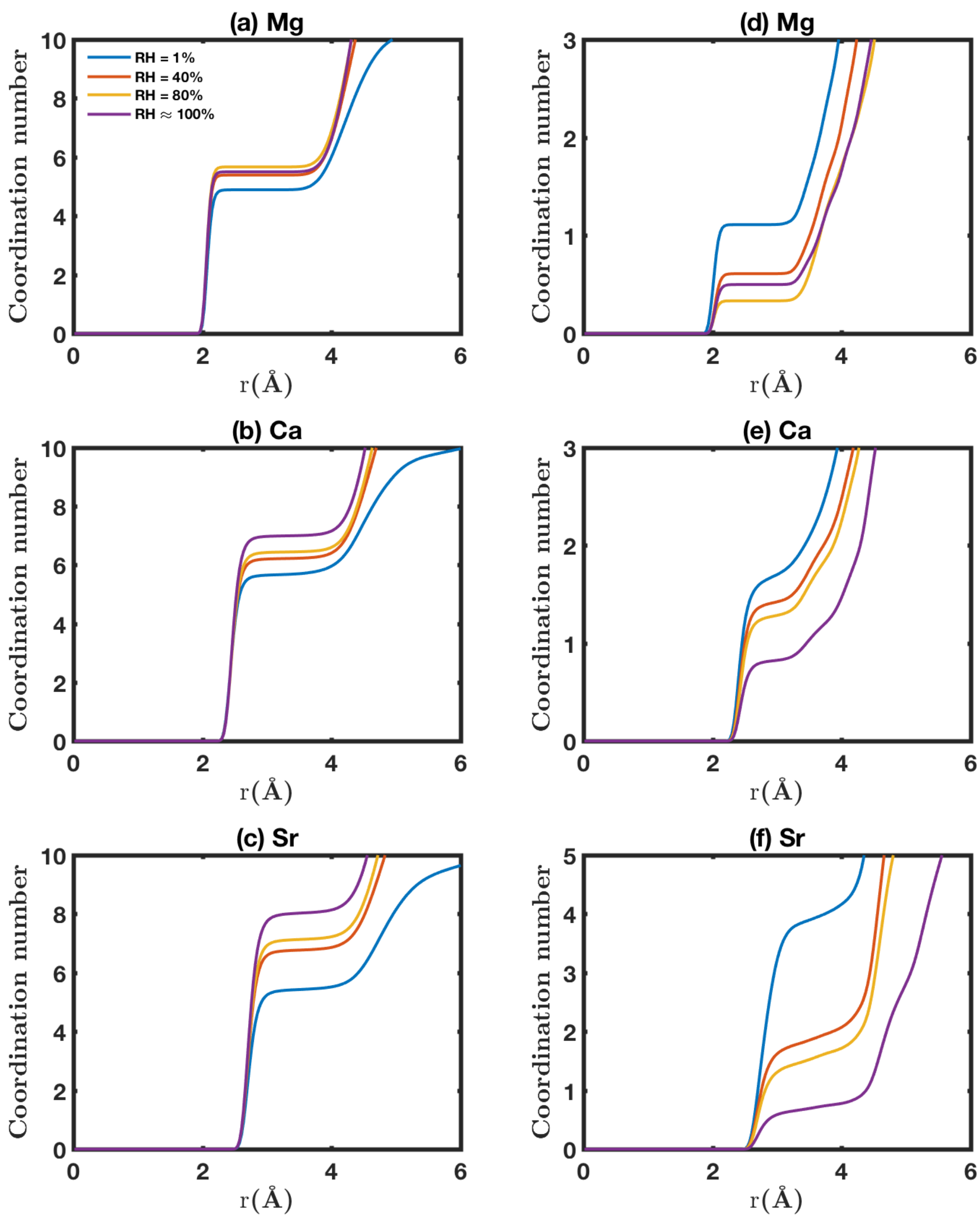

Figure S30: Same as in Fig. S14, but for Wyoming montmorillonite.

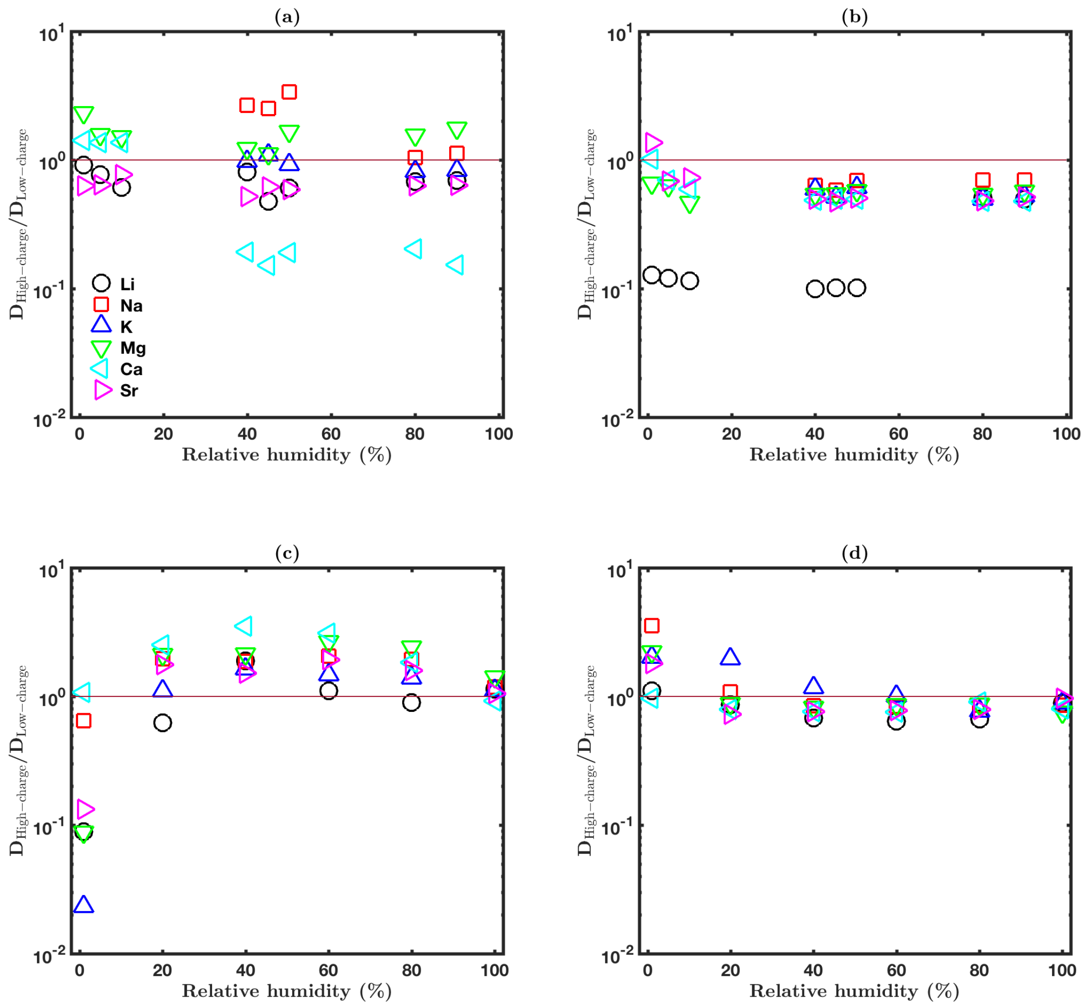

Figure S31: The ratio of diffusion coefficients for the ions (left panels) and water molecules (right panels) in the interlayers (top panels) and mesopore (bottom panels) at 298.15 K. (a) Ions in the interlayer, (b) water in the interlayer, (c) ions in the mesopore, and (d) water in the mesopore.